

## **Short title: Stomatal conductance under fluctuating light**

Author for correspondence:

*Sebastien Carpentier*

*Tel: +32(0)16 37 93 11*

*Email: [s.carpentier@cgiar.org](mailto:s.carpentier@cgiar.org)*

## **The impact of slow stomatal kinetics on photosynthesis and water use efficiency under fluctuating light**

David Eyland<sup>1</sup>, Jelle van Wesemael<sup>1</sup>, Tracy Lawson<sup>2</sup>, Sebastien Carpentier<sup>1,3</sup>

<sup>1</sup>Laboratory of Tropical Crop Improvement, Division of Crop Biotechnics, KU Leuven, Leuven, Belgium. <sup>2</sup>School of Life Sciences, University of Essex, Colchester, Essex, UK. <sup>3</sup>Bioversity International, Banana Genetic Resources, Leuven, Belgium.

### **One sentence summary**

Whole-plant transpiration rapidity corroborated leaf-level stomatal kinetics in banana, but impacts of stomatal dynamics under fluctuating light depended on other factors like time of day.

### **Author Contribution**

S.C. and T.L. supervised the experiments. D.E. performed the leaf gas exchange experiments. J.v.W. performed the whole-plant transpiration experiment. D.E., J.v.W., and S.C. analyzed the data. D.E., T.L. and S.C. wrote the manuscript. All authors reviewed and approved the final manuscript.

### **Funding information**

This work was funded by the Global TRUST foundation project “Crop wild Relatives Evaluation of drought tolerance in wild bananas from Papua New Guinea” (grant no: GS15024), by the CGIAR Research Program Roots, Tubers and Bananas (RTB-CRP), by the COST Action Phenomenall FA 1306 and by the Belgian Development Cooperation project “More fruit for food security: developing climate-smart bananas for the African Great Lakes region”.

## Abstract

Dynamic light conditions require continuous adjustments of stomatal aperture. The kinetics of stomatal conductance ( $g_s$ ) are hypothesized to be key to plant productivity and water use efficiency. Using step-changes in light intensity, we studied the diversity of light-induced  $g_s$  kinetics in relation to stomatal anatomy in five banana genotypes (*Musa* spp.) and modelled the impact of both diffusional and biochemical limitations on photosynthesis ( $A$ ). The dominant photosynthesis limiting factor was the diffusional limitation associated with  $g_s$  kinetics. All genotypes exhibited a strong limitation of  $A$  by  $g_s$ , indicating a priority for water saving. Moreover, significant genotypic differences in  $g_s$  kinetics and  $g_s$  limitations of  $A$  were observed. For two contrasting genotypes the impact of differential  $g_s$  kinetics was further investigated under realistic diurnally fluctuating light conditions and at whole-plant level. Genotype-specific stomatal kinetics observed at the leaf level were corroborated at whole-plant level by transpiration dynamics, validating that genotype-specific responses are still maintained despite differences in  $g_s$  control at different locations in the leaf and across leaves. However, under diurnally fluctuating light conditions the impact of  $g_s$  speediness on  $A$  and intrinsic water use efficiency ( $iWUE$ ) depended on time of day. During the afternoon there was a setback in kinetics: absolute  $g_s$  and  $g_s$  responses to light were damped, strongly limiting  $A$  and impacting diurnal  $iWUE$ . We conclude the impact of differential  $g_s$  kinetics depended on target light intensity, magnitude of change,  $g_s$  prior to the change in light intensity and particularly time of day.

## Introduction

In order to survive, plants need to balance CO<sub>2</sub> uptake for photosynthesis with water loss via transpiration. By adjusting their aperture, stomata control gaseous exchange between the leaf interior and the external atmosphere. Stomatal aperture is adjusted by moving solutes into or out of the guard cells. These changes in osmotic potential elicit water movement in or out of the guard cells, altering turgor pressure and subsequently aperture. In general, stomatal opening in well-watered C<sub>3</sub> and C<sub>4</sub> species is triggered by high light intensity, low vapour pressure deficit (VPD) and low CO<sub>2</sub> concentrations. Opposite environmental conditions (low light, high VPD and high [CO<sub>2</sub>]) stimulate stomatal closure (Assmann and Shimazaki, 1999; Outlaw, 2003; Lawson and Morison, 2004). Therefore, in a dynamic field environment, stomata are continuously adjusting aperture to achieve an appropriate balance between carbon gain and water loss (Percy, 1990; Lawson and Blatt, 2014). Most research has studied stomatal conductance ( $g_s$ ) and photosynthesis ( $A$ ) under steady-state conditions. A high  $g_s$  under steady-state conditions is associated with high  $A$  and consequently improved growth (Fischer et al., 1998; Franks, 2006). However, as  $g_s$  kinetics are typically a magnitude slower than those of  $A$ , the speed at which these steady-state values are reached in a fluctuating environment have a great influence on the growth and water use efficiency (Lawson and Blatt, 2014; Kaiser et al., 2016; McAusland et al., 2016; Taylor and Long, 2017; De Souza et al., 2020; Yamori et al., 2020). In a fluctuating field environment, light intensity is one of the most variable environmental conditions as it changes continuously by moving cloud covers and shading from adjacent plants (Percy, 1990; Slattery et al., 2018; Morales and Kaiser, 2020). In this way, stomata frequently experience alternating light intensities, inducing stomatal responses that change  $A$ ,  $g_s$  and the ratio of these, the intrinsic water use efficiency ( $\omega$ WUE). The balance between CO<sub>2</sub> gain and H<sub>2</sub>O loss under changing light intensities is disturbed by delayed  $g_s$  responses (Violet-Chabrand et al., 2017; Slattery et al., 2018). Limitations of  $A$  after an increase in light intensity are the combination of diffusional and biochemical limitations. Biochemical activation has been shown to majorly limit  $A$  during short lightflecks (Soleh et al., 2017; Taylor and Long, 2017; Acevedo-Siaca et al., 2020). Under longer light periods, limitations have been mainly attributed to stomatal limitations, with biochemical activation only limiting for a short time (< 10 min) because of rapid activation of RuBP regeneration and Rubisco (Mott and Woodrow, 2000; Kaiser et al., 2016; Deans et al., 2019a; De Souza et al., 2020). The slower  $g_s$  increase to increased light intensity limits the CO<sub>2</sub> uptake for

$A$ , while the slower  $g_s$  decrease to decreased light intensity results in unnecessary water loss. The limitation of  $A$  by the slower kinetics of  $g_s$  has been shown to be significant in well-watered C3 species (Farquhar and Sharkey, 1982; Jones, 1998; Lawson and Blatt, 2014; McAusland et al., 2016; Deans et al., 2019a). Rapid  $g_s$  kinetics therefore have been hypothesized to maximize  $A$  and  $i$ WUE, as steady-state values under the new conditions can be rapidly achieved (Lawson and Blatt, 2014; Papanatsiou et al., 2019; Kimura et al., 2020; De Souza et al., 2020). The  $g_s$  kinetics are, together with the final steady-state  $g_s$  the plant reaches, crucial to determine the plant performance (Franks and Farquhar, 2007; Vico et al., 2011; McAusland et al., 2016; Qu et al., 2016; Faralli et al., 2019b; Yamori et al., 2020). The importance of diversity in  $g_s$  kinetics was highlighted by De Souza et al. (2020), who showed a three-fold higher variability in carbon assimilation between cassava genotypes under fluctuating light than under steady-state conditions, mainly caused by differences in stomatal limitation. However, to our knowledge, the diversity of  $g_s$  kinetics across varieties has never been investigated at whole-plant level nor under diurnally fluctuating light conditions.

Here our research aimed to explore biodiversity in light-induced stomatal dynamics across genotypes and evaluate for the first time the impact on whole-plant level. We studied the diversity of light-induced  $g_s$  kinetics in relation to stomatal anatomy in five banana genotypes (*Musa* spp.) with distinct transpiration phenotypes (van Wesemael et al., 2019). We modelled the impact of diffusional and biochemical kinetics on  $A$  under single step-changes in light intensity and modelled the impact of differential  $g_s$  kinetics on  $A$  and  $i$ WUE under realistic diurnal fluctuating light conditions. By comparing the  $g_s$  kinetics in response to step-changes with the  $g_s$  responses under fluctuating light conditions, we gain insight into the importance of stomatal kinetics on diurnal carbon gain and water use efficiency.

## Results

### *A* and $g_s$ response to step-changes

Increasing light intensity from 100 to 1000  $\mu\text{mol m}^{-2} \text{s}^{-1}$  induced a strong stomatal opening response (Fig. 1). The  $g_s$  response followed a sigmoidal pattern. A similar sigmoidal limiting pattern was observed for *A* in all genotypes, indicating a strong limitation of *A* by  $g_s$  in banana (Fig. 1). Between genotypes there were significant differences in the speed of  $g_s$  increase. Steady-state *A* and  $g_s$  under high light intensity were reached in three out of five genotypes. In contrast, the genotypes Cachaco and Leite continued to increase  $g_s$  and *A* slowly after 90 min of 1000  $\mu\text{mol m}^{-2} \text{s}^{-1}$ . The subsequent decrease in light intensity from 1000 to 100  $\mu\text{mol m}^{-2} \text{s}^{-1}$  resulted in a rapid  $g_s$  decrease, which also followed a sigmoidal pattern (Fig. 1). Photosynthesis, on the other hand, as expected decreased instantly because light became the limiting factor (Fig. 1).

### Modelling steady-state & light-induced responses of $g_s$

The steady-state stomatal conductance at 100  $\mu\text{mol m}^{-2} \text{s}^{-1}$  ( $g_{s,100}$ ) and 1000  $\mu\text{mol m}^{-2} \text{s}^{-1}$  ( $g_{s,1000}$ ) did not differ significantly between genotypes (Fig. 2a, Supplemental Table S1).  $g_{s,100}$  ranged from 0.023 to 0.040  $\text{mol m}^{-2} \text{s}^{-1}$ , while  $g_{s,1000}$  ranged between 0.14 and 0.16  $\text{mol m}^{-2} \text{s}^{-1}$  (Fig. 2a, Supplemental Table S1).

The speed of  $g_s$  increase varied strongly between the banana genotypes and the modelled variables differed significantly (Fig. 2b-c, Supplemental Table S1). The genotype with the slowest  $g_s$  increase, Cachaco, had an average time constant  $K_i$  of 17 min, while the fastest genotype, Mbwazirume, had a  $K_i$  of 6.4 min (Fig. 2b, Supplemental Table S1). The speed of the decrease in  $g_s$  ( $K_d$ ) was also genotype-dependent (Fig. 2c, Supplemental Table S1).  $K_d$  was about 2 fold higher in Cachaco (9.5 min) than in Mbwazirume (4.4 min). Across all genotypes,  $K_i$  was significantly correlated with  $K_d$  ( $R^2 = 0.41$ ,  $P < 0.001$ ; Fig. 2d & Supplemental Fig. S1). However, the decrease in  $g_s$  was significantly faster than the increase ( $P < 0.001$ ).  $K_i$  was significantly correlated with the time to reach 95, 90 and 50% of steady-state  $g_s$  under the high light intensity ( $R^2 = 0.27 - 0.57$ ,  $P < 0.001$ ; Supplemental Fig. S1). Also the maximal slope of  $g_s$

increase and decrease ( $Sl_{max,i}$  and  $Sl_{max,d}$ ) were significantly correlated with the time constant  $K$  as the magnitude of  $g_s$  change was similar across genotypes ( $R^2 = 0.52$  &  $0.49$  for  $g_s$  increase and decrease respectively,  $P < 0.001$ ; Supplemental Fig. S1). During light-induced stomatal opening comparable differences across genotypes were present in  $Sl_{max,i}$  as in  $K_i$ . The lowest  $Sl_{max,i}$  values were observed for the genotype Cachaco and the highest values for Mbwarzirume (Supplemental Fig. S2, Supplemental Table S1).  $Sl_{max,d}$  was highest for the genotype Kluai Tiparot, while Leite showed the lowest  $Sl_{max,d}$  (Supplemental Fig. S2, Supplemental Table S1). Analogous to the opening and closing time constant, the absolute slope of closing was significantly higher than the opening slope ( $P < 0.001$ ).

### Impact of stomatal opening speed on $A$

The speed of the increase in  $g_s$  following a step-change in light intensity from  $100$  to  $1000 \mu\text{mol m}^{-2} \text{s}^{-1}$  strongly determined  $\text{CO}_2$  uptake during this period. The speed of changes in stomatal conductance in all genotypes accounted for more than 89 % of  $A$  limitation (Supplemental Fig. S3a). The time to reach 95% of steady-state  $A$  at  $1000 \mu\text{mol m}^{-2} \text{s}^{-1}$  ( $A_{1000}$ ) was greater than 30 min for almost all genotypes and differed significantly between Cachaco (51.9 min) and the genotypes Mbwarzirume (30.3 min) and Banksii (29.5 min) (Fig. 3a, Supplemental Fig. S4, Supplemental Table S2). This timing of  $A$  limitation was significantly correlated with the time to reach 95 %, 90 % and 50 % of steady-state  $g_s$  ( $P < 0.001$ ,  $R^2 = 0.42-0.48$ ), while there was no significant relation with the time to reach 95% or 90% of the maximum carboxylation rate of Rubisco ( $V_{cmax}$ , Supplemental Fig. S1, Supplemental Fig. S3). The timing to reach 95% of steady-state  $V_{cmax}$  was less than 20 minutes in all genotypes, while the timing to reach 95% of steady-state  $g_s$  was much longer and ranged between 41 and 69 minutes (Supplemental Fig. S3, Supplemental Table S2). The durations of  $A$  limitation was also significantly correlated with the modelled time constant for  $g_s$  increase ( $K_i$ ) ( $P < 0.001$ ,  $R^2 = 0.67$ , Supplemental Fig. S1). The percentage limitation of  $A$  was significantly higher in Cachaco (20.6 %) compared to the genotypes Mbwarzirume (10.2 %), Leite (10.2 %) and Banksii (8.5 %) (Fig. 3b) and was significantly related to both  $K_i$  and the time to reach 90 % and 50 % of steady-state  $g_s$ , confirming the impact of stomatal limitation on  $A$  (Supplemental Fig. S1).

### **$\dot{i}$ WUE response to step-changes in light intensity**

The step increase in light intensity induced an initial increase in  $A$  that was relatively larger than the increase in  $g_s$ . These responsiveness differences increased  $\dot{i}$ WUE, reaching the maximum  $\dot{i}$ WUE during the light period in all cases within 7.5 min (Supplemental Fig. S5). After reaching a maximal value,  $\dot{i}$ WUE decreased as both  $g_s$  and  $A$  gradually increased (Supplemental Fig. S5).  $\dot{i}$ WUE only stabilized when both  $A$  and  $g_s$  reached steady-state. The genotype Cachaco had a significantly higher mean  $\dot{i}$ WUE during the high light period compared to Mbwarzirume (Supplemental Fig. S6). The mean  $\dot{i}$ WUE during the high light period was significantly correlated with the time constant  $K_i$  and  $Sl_{max,i}$  with slower  $g_s$  responses resulting in higher  $\dot{i}$ WUE ( $R^2 = 0.12$  &  $0.42$ ,  $P < 0.05$ , Supplemental Fig. S1). The reduction in light intensity from 1000 to  $100 \mu\text{mol m}^{-2} \text{s}^{-1}$  instantaneously lowered  $\dot{i}$ WUE as  $A$  immediately declined because of light limitation (Supplemental Fig. S5). The mean  $\dot{i}$ WUE during this low light period was significantly higher in Kluai Tiparot, than in Leite (Supplemental Fig. S6). The mean  $\dot{i}$ WUE was significantly correlated to the stomatal closing variables  $K_d$  and  $Sl_{max,d}$  with faster  $g_s$  responses resulting in higher  $\dot{i}$ WUE ( $R^2 = 0.36$  &  $0.26$ ,  $P < 0.001$ , Supplemental Fig. S1).

### **Stomatal anatomy**

Banana has elliptical-shaped guard cells surrounded by four to six subsidiary cells (Rudall et al., 2017). Abaxial stomatal density, stomatal length, guard cell size and subsidiary cell size were quantified from the leaf part enclosed in the gas exchange cuvette and significant differences between genotypes were observed (Supplemental Fig. S7). Stomatal density and stomatal length were not correlated with any of the modelled light-induced  $g_s$  kinetics (Fig. 4, Supplemental Fig. S1). However, these correlations between anatomy and  $g_s$  kinetics were significant if the genotype Cachaco with lowest  $g_s$  rapidity was not considered (Fig. 4). In this case, stomatal density was significantly correlated with the time constant  $K$  as well as the maximum slope of  $g_s$  response  $Sl_{max}$  during both stomatal opening and closing ( $P < 0.01$ ;  $R^2 = 0.25 - 0.46$ ).

### **Whole-plant transpiration response at dawn**

The significant differences in  $g_s$  speed at leaf level observed between the two extreme genotypes Cachaco and Mbwarzirume were confirmed at the whole-plant level under a step increase in light intensity from darkness (Fig. 5) and under a gradually increasing light intensity (Supplemental

Fig. S8). After the onset of light in the morning, transpiration rate increased significantly faster in Mbwarzirume compared to Cachaco (Fig. 5a-b, Supplemental Fig. S8a). After a step increase in light intensity, a significant increase in transpiration rate was observed after *c.* 15 min in Mbwarzirume, while in Cachaco this was only after 25 min (Fig. 5a-b). Similar faster increases in transpiration rate of Mbwarzirume were observed under a gradually increasing light intensity (Supplemental Fig. S8a). The temporal response of whole-plant transpiration rate to a step increase in light intensity was also modelled following the sigmoidal model (Eqn. 1) and the time constants  $K_i$  differed significantly between genotypes (Supplemental Fig. S9). Similar to the response at leaf level, Cachaco, had an average time constant  $K_i$  of 20 min, while Mbwarzirume, had a  $K_i$  of 8.5 min (Supplemental Fig. S9). The difference in transpiration responses was also reflected in the transpiration rate before and after dawn. The whole plant transpiration rate did not differ significantly between both genotypes pre-dawn, but after the step change in light intensity, the transpiration rate was significantly higher in Mbwarzirume for 90 minutes, whereafter both genotypes reached similar steady-state transpiration rates (Fig 5b). Likewise, the transpiration rate under gradually increasing light intensity did not differ pre-dawn, but was significantly higher in Mbwarzirume after the onset of light (Supplemental Fig. S8b).

### Impact of diurnal light fluctuations on $g_s$ , $A$ and $iWUE$

To evaluate the impact of  $g_s$  kinetics on diurnal  $A$  and  $iWUE$ , plants were subjected to fluctuating light intensities and phenotyped over an entire diurnal period. Similar to the transpiration rate measured at the whole-plant level, the morning increase in  $g_s$  at leaf-level under gradually increasing light intensity was faster in Mbwarzirume compared to Cachaco (Fig. 6a). The time constant for the  $g_s$  increase ( $K_i$ ) was significantly higher in Cachaco ( $P < 0.005$ , Fig. 6b). However, the faster increase of  $g_s$  in Mbwarzirume, did not result in increased  $A$  (Fig. 6c). Maximum potential  $A$  values at specific light intensities were determined from light response curves and compared to those measured under the diurnal conditions. Under the gradual increasing light intensities experienced in the morning, maximum  $A$  values were achieved, indicating there was no  $g_s$  limitation under these light-limiting conditions (Fig. 7). A similar  $A$  with lower  $g_s$  during the morning, led to a significantly higher mean  $iWUE$  in Cachaco ( $P < 0.05$ , Fig. 6d).



Throughout the day,  $g_s$  kinetics were in most cases significantly faster for the genotype Mbwazirume compared to Cachaco (Fig. 8a), again confirming the previously observed kinetics (Fig. 2, Fig. 5). However, under fluctuating light conditions  $g_s$  kinetics were dependent on the magnitude of light intensity change,  $g_s$  values prior to the light intensity change and the time of the day (Fig. 8a). During the afternoon there was a setback in kinetics: the absolute  $g_s$  and the  $g_s$  responses to light were damped (Fig.7, Fig. 8). Simultaneously  $A$  decreased greatly in the afternoon, which could be mainly attributed to a reduction in  $g_s$ . The limitation of  $A$  in the afternoon was three times higher in Cachaco (52.6 %) compared to Mbwazirume (17.5 %) (Fig. 7, Fig. 9d). The reduction of  $g_s$  in the afternoon resulted in a significantly lower average diurnal  $g_s$  (Fig. 9a) which translated into a greater diurnal  $iWUE$  in Cachaco compared to Mbwazirume (Fig.8c, Fig. 9c).

## Discussion

### Stomatal behaviour greatly limits photosynthesis in banana

Step-changes in light intensity have shown to induce an uncoupling of  $A$  and  $g_s$  in many species (Barradas and Jones, 1996; Lawson and Blatt, 2014; McAusland et al., 2016; Faralli et al., 2019a). However, all banana genotypes maintain a tight coupling between  $A$  and  $g_s$  following a step increase in light intensity (Fig. 1). This indicates a strong stomatal control of photosynthesis, which is demonstrated by diffusional limitations accounting for over 89 % of  $A$  limitation (Supplemental Fig. S3a). This high stomatal limitation of  $A$  is explained by the slow  $g_s$  response (Fig. 1, Fig. 2) relative to the faster biochemical activation. The time required for biochemical activation was much lower and not correlated with the time for steady-state  $A$  and  $g_s$  (Supplemental Fig. S3). Similar to Deans et al. (2019a) and De Souza et al. (2020), the speed of changes in  $g_s$  was the predominant limitation of  $A$ . This behaviour shows that banana strongly controls stomatal aperture, resulting in water conservation at the expense of potential carbon gain, which supports the early work of Aubert and Catsky (1970). This prioritizing of water conservation in banana can be explained by its intrinsic need to maintain a high leaf water potential (Turner and Thomas, 1998).

### Diversity in light-induced stomatal responses

Stomatal responses to changes in light intensity have been shown to vary at an inter- and intra-specific level (Vico et al., 2011; Drake et al., 2012; McAusland et al., 2016; Qu et al., 2016; Durand et al., 2020; De Souza et al., 2020). A higher steady-state  $g_s$  has been linked with faster light-induced  $g_s$  responses (Drake et al., 2012; Kaiser et al., 2016; McAusland et al., 2016; Wachendorf and Küppers, 2017; Sakoda et al., 2020). Although the differences observed in steady-state  $g_s$  values between banana genotypes were not significant, their  $g_s$  kinetics differed strongly (Fig. 2). These results suggest that other factors such as stomatal anatomy, hydraulic conductance and membrane transporters are involved in determining the rapidity of changes in  $g_s$ .

The banana B genome is often related to drought tolerance because of its center of origin and its natural occurrence in drier habitats under full sunlight (Perrier et al., 2011; Janssens et al., 2016; Eyland et al., 2021). Within the investigated banana genotypes we observed significant differences in the speed of increase and decrease in  $g_s$  (Fig. 2b,c). However, differences across

genotypes were not explained by their genomic constitution (see Materials & Methods), which is in agreement with the wide diversity of transpiration phenotypes observed irrespective of genomic constitution (van Wesemael et al., 2019).

Consistent with previous works in other species (Vico et al., 2011; McAusland et al., 2016; Faralli et al., 2019a), the speed of  $g_s$  increase and decrease were significantly correlated (Fig. 2d). Decreases in  $g_s$  were faster than opening in all banana genotypes (Fig. 2d), which is not the case for all crops (McAusland et al., 2016; Qu et al., 2016). The faster  $g_s$  closure again indicates that banana prioritises water conservation over maximization of carbon uptake.

The two most extreme genotypes Cachaco and Mbwazirume, with the slowest and fastest  $g_s$  responses respectively, also showed at the whole-plant level differences in the light-induced speed of transpiration rate increase (Fig. 5, Supplemental Fig. S8, Supplemental Fig. S9). This finding suggests that despite possible differences in  $g_s$  control of water loss at different locations of the leaf (Matthews et al., 2017) and across leaves of different age (Urban et al., 2008) genotype-specific responses are still maintained. Leaf level measurements of light-induced  $g_s$  kinetics are thus in line with whole-plant responses. To our knowledge, this is the first report confirming stomatal kinetics at the whole-plant level. The genotype-specific difference in whole-plant transpiration responses at dawn was validated at the leaf level with  $g_s$  increasing faster in Mbwazirume under gradually increasing light intensity (Fig. 6a). This faster  $g_s$  increase in Mbwazirume did not result in higher  $A$ , indicating that at dawn, under gradually increasing low light intensities,  $g_s$  was not limiting  $A$  and was higher than necessary for maximal  $A$  (Fig. 6 & Fig. 7). These results demonstrate that the impact of  $g_s$  kinetics on  $A$  and  $iWUE$  depend on the time of the day and the light conditions. The uncoupling of  $g_s$  and  $A$  under increasing light conditions at dawn was not beneficial for carbon uptake. Gosa et al. (2019) called this period after dawn in tomato the golden hour because in dry climates it is the time of the day with the highest  $g_s$ . Later in the day, VPDs become too high, restricting  $g_s$  (Gosa et al., 2019). Breeding for an even higher  $g_s$  during this golden hour was suggested to improve plant productivity. However, care must be taken to breed for an improved morning  $CO_2$  uptake, rather than for a high  $g_s$  with associated uncoupling of  $A$  and  $g_s$ . Although the absolute water loss resulting from excessive morning  $g_s$  might be relatively low because of low evaporative demands at dawn (Chaves et al., 2016), it may lead to a crucial decrease in overall plant water status.

Despite the confirmed genotypic differences in stomatal kinetics, the impact of  $g_s$  kinetics on  $A$  and  $iWUE$  before noon hardly differed between the genotypes Cachaco and Mbwarzirume under field-mimicking light conditions (Fig. 7, Fig. 8). This could be explained by lower amplitudes of light switches compared to a single step-change in light intensity and/or  $g_s$  values not being at steady-state prior to changing light intensity. The genotype-specific speed of the  $g_s$  response observed under a single step-change in light intensity did not explain the diurnal  $iWUE$ , indicating that  $g_s$  kinetics only partially affect diurnal water use efficiency and carbon gain (Fig. 9b,c). The absolute  $g_s$  and the  $g_s$  responses to light decreased strongly in the afternoon, and this effect was more pronounced in the genotype Cachaco (Fig. 7, Fig. 8a). The three times higher afternoon limitation of  $A$  in the genotype Cachaco compared to Mbwarzirume, resulted in a significant higher diurnal  $iWUE$  (Fig. 9c,d). The genotype Cachaco with the slowest  $g_s$  kinetics thus achieved the highest  $iWUE$ , showing that not only  $g_s$  speed but also the  $g_s$  diurnal pattern determines the overall water use efficiency and carbon gain. Although the mechanism behind the afternoon  $g_s$  reduction remains largely unknown, it is commonly hypothesized to be related to circadian regulation of ABA sensitivity and associated endogenous signals regulating the clock, such as feedback loops from photosynthate accumulation (Mencuccini et al., 2000; Haydon et al., 2013; Delorge et al., 2014; Resco de Dios and Gessler, 2018). We show that under fluctuating light conditions this intrinsic diurnal pattern of absolute  $g_s$  decrease and  $g_s$  light responsivity reduction is decisive for diurnal  $iWUE$  (Fig. 9c).

### Impact of stomatal anatomy on responses

Stomatal density as well as the size have been reported to affect  $g_s$  kinetics (Hetherington and Woodward, 2003; Drake et al., 2012; Raven, 2014; Sakoda et al., 2020). However, McAusland et al. (2016) and Faralli et al. (2019a) reported no or only a weak inter- and intra-specific correlation between stomatal anatomy and light-induced  $g_s$  kinetics. We confirmed that stomatal density and size were not correlated with the  $g_s$  kinetics (Fig. 4, Supplemental Fig. S1). Remarkably, the genotype with the slowest increase in  $g_s$ , Cachaco had the second highest density and the smallest stomata. Without this genotype a significant correlation between density and the speed of  $g_s$  increase and decrease was observed (Fig. 4). This exception suggests that the surface-to-volumes ratios are not always directly related to stomatal speed as this assumes uniform ion transport activity per surface area (Lawson and Blatt, 2014).

## Conclusion

Our findings show that there is diversity in  $g_s$  rapidity to light within closely related banana genotypes and that slow stomatal responses and not biochemical activation greatly limit  $A$ . The priority of banana for water saving is shown by strong stomatal control of  $A$  and faster decrease in  $g_s$  than increase. The observed diversity in  $g_s$  rapidity was not related to stomatal anatomy and therefore suggests that variation is rather driven by functional components. We show here for the first time that the  $g_s$  rapidity observed at the leaf level can also be found at the whole-plant level. However, under fluctuating light conditions,  $g_s$  rapidity is only one of the many physiological factors determining overall plant water use efficiency and carbon gain.

## Materials & methods

### Experiment 1: Leaf gas exchange response to a step-change in light intensity

#### Plant material and growth conditions

Banana plants (*Musa* spp.) were obtained through the International Musa Transit Center (ITC, Bioversity International), hosted at KU Leuven, Belgium. Plants of five genotypes from different subgroups were selected: Banksii (subgroup Banksii, AA genome, ITC0623), Cachaco (Bluggoe, ABB genome, ITC0643), Kluai Tiparot (Kluai Tiparot, ABB genome, ITC0652), Leite (Rio, AAA genome, ITC0277) and Mbwazirume (Mutika-Lujugira, AAA genome, ITC1356). Plants were grown in 800 ml containers filled with peat-based compost (Levingtons F2S, UK) under  $350 \mu\text{mol m}^{-2} \text{s}^{-1}$  Photosynthetic Photon Flux Density (PPFD) in a 12 h : 12 h light : dark cycle with temperature and relative humidity at  $26 \pm 1 \text{ }^\circ\text{C}$  and  $70 \pm 10 \%$ , respectively. Plants were well-watered and starting from week three a Hoagland nutrient solution was added. Measurements were performed when plants were fully acclimated and seven weeks old.

#### Leaf gas exchange measurements

Photosynthetic rate ( $A$ ) and stomatal conductance to water ( $g_s$ ) were measured every 30 s on the middle of the second youngest fully developed leaf using a LI-6400XT infrared gas analysis and dew-point generator model LI-610 (LI-COR, USA). Light was applied by an integrated LED light source. The leaf cuvette maintained a  $\text{CO}_2$  concentration of  $400 \mu\text{mol mol}^{-1}$ , a leaf temperature of  $25^\circ\text{C}$  and a VPD of 1 kPa. All measurements were performed before 14:00 h to avoid circadian influences.

#### Stomatal response to a step-change in light intensity

The light intensity was kept at  $100 \mu\text{mol m}^{-2} \text{s}^{-1}$  until  $A$  and  $g_s$  were stable for 10 min. Once steady-state was reached, light intensity was increased to  $1000 \mu\text{mol m}^{-2} \text{s}^{-1}$  for 90 min. Then, light intensity was lowered back to  $100 \mu\text{mol m}^{-2} \text{s}^{-1}$  for 30 min.

The increase in  $g_s$  after the increase in light intensity and the decrease in  $g_s$  after the decrease in light intensity followed a sigmoidal pattern and was modelled using the non-linear sigmoidal model described in Violet-Chabrand et al. (2017):

$$g_s = (g_{s,1000} - g_{s,100}) e^{-e^{\left(\frac{\lambda-1}{K}+1\right)}} + g_{s,100} \quad (\text{Eqn. 1})$$

With  $g_s$  the stomatal conductance at time  $t$ ,  $K$  the time constant for rapidity of  $g_s$  response (min),  $\lambda$  the lag time of the sigmoidal curve (min),  $g_{s,100}$  and  $g_{s,1000}$  ( $\text{mol m}^{-2} \text{s}^{-1}$ ) the steady-state  $g_s$  at 100 and 1000  $\mu\text{mol m}^{-2} \text{s}^{-1}$  respectively. Parameter values were estimated for each individual plant using non-linear model optimization in R (V 3.4.3).  $K_i$  indicates the  $g_s$  increase time constant,  $K_d$  the  $g_s$  decrease time constant. The maximum slope of  $g_s$  during opening and closing was calculated and defined as  $Sl_{max}$ . Intrinsic water use efficiency ( $i\text{WUE}$ ) was calculated as  $i\text{WUE} = A/g_s$ . Outlying values (0.5 % quantile;  $i\text{WUE} < 0$  or  $> 400 \mu\text{mol mol}^{-1}$ ) caused by low  $g_s$  were discarded for plotting.

### Stomatal and biochemical limitation analysis

Photosynthesis was considered to be limited until 95 % of steady-state  $A$  at 1000  $\mu\text{mol m}^{-2} \text{s}^{-1}$  was reached (McAusland et al., 2016). The percentage of limitation of  $A$  was calculated by comparing the measured  $A$  with the maximal steady-state  $A$  under 1000  $\mu\text{mol m}^{-2} \text{s}^{-1}$  according to McAusland et al., (2016):

$$\text{Limitation of } A \text{ (\%)} = \frac{\int_0^t \Sigma(A_{max} - A_{measured})}{\int_0^{90} \Sigma A_{measured}} \quad (\text{Eqn. 2})$$

With  $A_{max}$  the value reached at 95 % of steady-state  $A$  under 1000  $\mu\text{mol m}^{-2} \text{s}^{-1}$ ,  $A_{measured}$  the measured  $A$  and  $t$  the time where 95 % of steady-state  $A$  is reached.

The delay in obtaining maximum potential  $A$  under 1000  $\mu\text{mol m}^{-2} \text{s}^{-1}$  is determined by the stomatal opening speed as well as the rate of biochemical activation. The activation rate of Rubisco is the main biochemical limiting component during step changes in light exceeding several minutes (Mott and Woodrow, 2000; Way and Percy, 2012). To quantify the relative contributions of biochemical and stomatal limitations a differential method was applied (Jones, 1985; Wilson et al., 2000; Grassi and Magnani, 2005; Deans et al., 2019b). As explained by Deans et al. (2019b), the forgone  $A$  because of biochemical and stomatal limitation was calculated as:

$$dA_{biochem} = \frac{\partial A}{\partial v_{cmax}} dv_{cmax} \quad (\text{Eqn. 3})$$

and

$$dA_{stom} = \frac{\partial A}{\partial g_{sc}} dg_{sc} \quad (\text{Eqn. 4})$$

Where  $V_{cmax}$  is the maximum velocity of Rubisco for carboxylation and  $g_{sc}$  the stomatal conductance to  $CO_2$ .  $V_{cmax}$  at every time point was calculated by solving the Rubisco-limited photosynthesis as described by Farquhar et al., (1980) for  $V_{cmax}$ :

$$V_{cmax} = \frac{(A+R_d)(C_i+K_m)}{(C_i-\Gamma^*)} \quad (\text{Eqn. 5})$$

Where  $C_i$  is the  $CO_2$  concentration in the intercellular airspaces of the leaf.  $R_d$  represents the mitochondrial respiration for which average dark respiration rates were used.  $\Gamma^*$  is the photorespiratory compensation point and  $K_m$  is the effective the Rubisco Michaelis-Menten constant for  $CO_2$  under 21%  $O_2$ . Values for  $\Gamma^*$  and  $K_m$  were taken as the average for C3 species at 25°C as described by Hermida-Carrera et al. (2016), 41.2 and 529.4  $\mu\text{mol mol}^{-1}$  respectively. Mesophyll conductance to  $CO_2$  was assumed to be infinite.  $g_{sc}$  at every time point was calculated as:

$$g_{sc} = \frac{g_s}{1.6} \quad (\text{Eqn. 6})$$

The relative stomatal limitation ( $\sigma_{stom}$ ) was then calculated as:

$$\sigma_{stom} = \frac{\int_0^t dA_{stom} dt}{\int_0^t dA_{biochem} dt + \int_0^t dA_{stom} dt} \quad (\text{Eqn. 7})$$

Where  $t$  represents the time where 95 % of steady-state  $A$  under 1000  $\mu\text{mol m}^{-2} \text{s}^{-1}$  was reached. Timings representing the  $g_s$  and  $A$  increase were calculated at 95, 90 and 50% of steady-state values under 1000  $\mu\text{mol m}^{-2} \text{s}^{-1}$ . Timings for  $V_{cmax}$  were calculated at 95 and 90% of steady-state values.

### Stomatal anatomy measurements

Stomatal impressions of the abaxial surface of the leaf were made when stomata were completely closed using impression material. Impressions were made by applying dental polymer according to the protocol of Weyers & Johansen (1985), followed by covering the polymer with nail varnish and placement on a microscope slide. Impressions were only taken from the abaxial side, because stomatal densities are generally 75 % higher compared to the adaxial side in banana, therefore majorly determining gas exchange as shown by Brun (1961). Stomatal anatomy was quantified using an EVOS digital inverted microscope. Stomatal density was determined in three microscopic field of views of 1.12  $\text{mm}^2$  captured with a 10 x objective lens (54 to 117 stomata



per field of view). Guard cell length ( $\mu\text{m}$ ), guard cell size ( $\text{mm}^2$ ) and lateral subsidiary cell size ( $\text{mm}^2$ ) were determined in three microscopic field of views of  $0.07 \text{ mm}^2$  captured with a 40 x magnification respectively (four to seven stomata per field of view). Measurements were performed in ImageJ software (<http://rsb.info.nih.gov/ij>).

## Experiment 2: Whole-plant transpiration response at dawn

### Plant material and growth conditions greenhouse experiment

For the genotypes Cachaco and Mbwazirume, 12 plants were grown for seven weeks in a greenhouse prior to the experiment. Plants were grown in 10 l containers filled with peat-based compost. At the start of the experiments, the six most homogenous plants per genotype were selected based on leaf area. Weight of each plant was followed by a multi-lysimeter setup of high precision balances, registering the weight every 60 seconds (1 g accuracy, Phenospex, Heerlen, NL). The soil was covered by plastic to avoid evaporation and ensure only waterloss through transpiration. The transpiration rate was calculated by differentiating the raw weight data over time. The soil water content was determined by subtracting the plastic pot weight, the dry soil weight and the plant weight from the total weight measurement. Dry soil weight was calculated as a function of the soil volume (bulk density =  $0.2267 \text{ g cm}^{-3}$ ). Leaf area was calculated by weekly top view imaging and modelled over time by a power law function (Paine et al., 2012):

$$\text{leaf area} = k + a * \text{days}^b \quad (\text{Eqn. 8})$$

The daily plant weight was estimated from the projected leaf area using genotype-specific correlations ( $n > 50$ ;  $R^2 \geq 0.94$ ). Plants were watered with a nutrient solution during the night and kept at well-watered conditions. Radiation was collected every 5 min via a sensor (Skye instruments, UK) inside the greenhouse. Supplemental lighting of  $14 \text{ W m}^{-2}$  at plant level was provided when solar radiation was below  $250 \text{ W m}^{-2}$  during the daytime. Temperature and relative humidity data were collected using six data loggers (Trotec, DE) registering data every 5 min. The onset of light was defined as the moment when intensity increased above  $2 \text{ W m}^{-2}$ .

### Plant material and growth conditions controlled environment experiment

For the genotypes Cachaco and Mbwazirume, three plants were grown in a growth chamber with relative humidity of 70 % and temperature of  $24 \text{ }^\circ\text{C}$ . Plants were grown hydroponically in containers with 350 ml medium (see van Wesemael et al. (2019) for specific nutrient composition) and placed under adjustable LED panels (LuminiGrow 600R1, Lumini technology

Co. Ltd., China) providing  $120 \mu\text{mol m}^{-2} \text{s}^{-1}$  in a 12 h/12 h light/dark cycle. Plants were 5 weeks old at the start of the experiment and weighted prior to the experiment to normalize for plant mass. Biomass was again measured after 8 days, at the end of the experiment. Water loss of each plant was followed by a multi-lysimeter setup of high precision balances (0.01 g accuracy, Kern, Germany). Balances were connected to a computer registering the weight every 10 seconds.

### Experiment 3: Impact of diurnal light fluctuations on $g_s$ , $A$ and $iWUE$

#### Plant material and growth conditions

Four plants of the genotypes Cachaco and Mbwarzirume were grown in a greenhouse. Plants were grown in 4 l containers filled with peat-based compost and maintained under well-watered conditions. After 8 weeks plants were moved to a growth chamber with relative humidity  $70 \pm 15 \%$  and temperature  $28 \pm 2 \text{ }^\circ\text{C}$ .

#### Leaf gas exchange measurements

$A$  and  $g_s$  were measured every minute on the middle of the second youngest fully developed leaf using a LI-6800 infrared gas analyser (LI-COR, USA). The leaf cuvette maintained a  $\text{CO}_2$  concentration of  $400 \mu\text{mol mol}^{-1}$ , a leaf temperature of  $28 \text{ }^\circ\text{C}$  and a VPD of 1 kPa. The light intensity was programmed to fluctuate throughout the day. Plants were placed under adjustable LED panels (LuminiGrow 600R1, Lumini technology Co. Ltd., China) that mimicked light fluctuations inside the LI-6800 leaf cuvette. The  $g_s$  response was described using the non-linear sigmoidal model of Vialet-Chabrand et al. (2013) where light or dark steps were sufficiently long for model optimization (Eqn. 1). A light response curve with  $A$  in function of photosynthetic photon flux density (PPFD) was modelled for each individual based on  $A$  values recorded during the first six hours of the day that were not limited by  $g_s$ . The nonrectangular hyperbola-based model of Prioul & Chartier (1977) was optimized as described by Lobo et al. (2013):

$$A = \frac{PPFD * \Phi_0 + A_{max} - \sqrt{(\Phi_0 * PPFD + A_{max})^2 - 4\theta * \Phi_0 * PPFD * A_{max}}}{2\theta} - R_n \quad (\text{Eqn.9})$$

With  $A$  the photosynthetic rate ( $\mu\text{mol m}^{-2} \text{s}^{-1}$ ), PPFD the Photosynthetic Photon Flux Density ( $\mu\text{mol m}^{-2} \text{s}^{-1}$ ),  $\Phi_0$  the quantum yield at PPFD of  $0 \mu\text{mol m}^{-2} \text{s}^{-1}$  ( $\mu\text{mol } \mu\text{mol}^{-1}$ ),  $A_{max}$  the absolute maximum photosynthetic rate ( $\mu\text{mol m}^{-2} \text{s}^{-1}$ ),  $\theta$  the dimensionless convexity factor and  $R_n$  the dark respiration ( $\mu\text{mol m}^{-2} \text{s}^{-1}$ ).

The percentage of limitation of  $A$  by  $g_s$  during the afternoon ( $> 6$  hours after light onset) was calculated by estimating the maximal potential  $A$  without  $g_s$  limitation and comparing it with the measured  $A$  (Eqn. 2).

### Statistical analysis and data processing

All data processing and statistical analysis was carried out in R (V 3.4.3). Genotypic differences were tested by applying one-way analysis of variance (ANOVA) with a post hoc Tukey HSD test. Segmented regression was performed on the whole-plant transpiration between -90 and 90 min relative to the onset of light. Data with no significant segmented regression (p-value Davies Test  $< 0.05$ , segmented R package, 7.5% of the data) and negative slopes (2.5% of the data) were removed. Transpiration rate was calculated as the mean water loss every 30 min. To use the sigmoidal model (Eqn. 1) on whole-plant transpiration data, 1 min weight measurements were smoothed according to the Savitzky and Golay (1964) method with a filtering window of 21 and a fourth-order polynomial. Each day of whole-plant transpiration responses was regarded as a new replicate by incorporating a plant-specific factor and a date-specific factor as a random effect in a linear mixed model.

### Supplemental Data

**Supplemental Fig. S1** Correlation matrix of gas exchange and stomatal anatomy variables.

**Supplemental Fig. S2** Maximum slope of stomatal conductance response ( $Sl_{max}$ ) to an increase in light intensity from  $100 \mu\text{mol m}^{-2} \text{s}^{-1}$  to  $1000 \mu\text{mol m}^{-2} \text{s}^{-1}$  and to a decrease in light intensity from  $1000 \mu\text{mol m}^{-2} \text{s}^{-1}$  to  $100 \mu\text{mol m}^{-2} \text{s}^{-1}$

**Supplemental Fig. S3** Stomatal limitation of photosynthesis ( $A$ ) and timings until steady-state values of stomatal conductance ( $g_s$ ), photosynthesis and maximum velocity of Rubisco for carboxylation ( $V_{cmax}$ ) were reached after an increase in light intensity from  $100 \mu\text{mol m}^{-2} \text{s}^{-1}$  to  $1000 \mu\text{mol m}^{-2} \text{s}^{-1}$ .

**Supplemental Fig. S4** Increase in photosynthesis ( $A$ ) after increasing the light intensity from  $100 \mu\text{mol m}^{-2} \text{s}^{-1}$  to  $1000 \mu\text{mol m}^{-2} \text{s}^{-1}$ .  $A$  was considered limited until 95 % of steady-state  $A$  was reached.

**Supplemental Fig. S5** Response of intrinsic water use efficiency ( $iWUE$ ) and the intracellular  $CO_2$  ( $C_i$ ) to a step increase and decrease in light intensity from 100 to 1000  $\mu mol m^{-2} s^{-1}$  and back.

**Supplemental Fig. S6** Mean intrinsic water use efficiency ( $iWUE$ ) after the increase in light intensity from 100 to 1000  $\mu mol m^{-2} s^{-1}$  and the decrease to 100  $\mu mol m^{-2} s^{-1}$  afterwards.

**Supplemental Fig. S7** Stomatal density, stomatal length, guard cell size, subsidiary cell size and proportion of subsidiary cells of the five banana genotypes.

**Supplemental Fig. S8** Gravimetric transpiration rate analysis of genotypes Cachaco and Mbwazirume under gradual increasing light intensity.

**Supplemental Fig. S9** Modelled time constant ( $K_i$ ) for the whole-plant transpiration rate increase of genotypes Cachaco and Mbwazirume after a step increase in light intensity from 0 to 120  $\mu mol m^{-2} s^{-1}$ .

**Supplemental Table S1** Modelled steady-state and light-induced variables of the stomatal conductance ( $g_s$ ) response to a step increase and decrease in light intensity from 100 to 1000  $\mu mol m^{-2} s^{-1}$  for five different banana genotypes.

**Supplemental Table S2** Time to reach 95%, 90% and 50% of steady-state photosynthesis ( $A$ ), stomatal conductance ( $g_s$ ) and  $V_{cmax}$  after a step increase in light intensity from 100 to 1000  $\mu mol m^{-2} s^{-1}$  for five different banana genotypes.

## Acknowledgement

The authors would like to thank Edwige André for the plant propagation and growth; Hendrik Siongers, Stan Blomme, Loïck Derette, Simon Costers and Kaat Hebbelinck for technical assistance during plant growth and phenotyping; Silvere Vialet-Chabrand and Phil Davey for their technical assistance during the step-changes in light intensity experiment.

## Figure legends

**Fig. 1** Response of stomatal conductance ( $g_s$ , orange) and photosynthesis ( $A$ , black) of five banana genotypes to a step increase in light intensity from 100 to 1000  $\mu\text{mol m}^{-2}\text{s}^{-1}$  followed by a decrease from 1000 to 100  $\mu\text{mol m}^{-2}\text{s}^{-1}$ . Grey and white areas indicate time periods of 100  $\mu\text{mol m}^{-2}\text{s}^{-1}$  and 1000  $\mu\text{mol m}^{-2}\text{s}^{-1}$ , respectively. Dashed lines indicate when 95 % of steady-state  $A$  was reached. Points and error bars represent mean  $\pm$  SE ( $n = 7-8$ ).

**Fig. 2** Modelled steady-state and light-induced variables of the stomatal conductance ( $g_s$ ) response to a step increase and decrease in light intensity between 100 and 1000  $\mu\text{mol m}^{-2}\text{s}^{-1}$  for five different banana genotypes ( $n = 7-8$ ). (A) Steady-state  $g_s$  at 100 ( $g_{s,100}$  faded colours) and 1000  $\mu\text{mol m}^{-2}\text{s}^{-1}$  ( $g_{s,1000}$  bold colors). (B) Time constant of  $g_s$  increase ( $K_i$ ) for different genotypes. Different letters indicate significant differences between genotypes (post hoc Tukey HSD test,  $P < 0.05$ ;  $A > B > C$ ). (C) Time constant of  $g_s$  conductance decrease ( $K_d$ ) for different genotypes. Different letters indicate significant differences between genotypes (post hoc Tukey HSD test,  $P < 0.05$ ;  $A > B > C$ ). (D) Significant correlation between  $K_i$  and  $K_d$  (Pearson's correlation,  $R^2 = 0.41$ ,  $P < 0.001$ ).  $K_i$  was significantly higher than  $K_d$ . The solid line shows the linear regression, the dashed line shows the 1:1 line. Points and error bars represent mean  $\pm$  SE ( $n = 7-8$ ). The bold middle line in boxplots represents the median. The box is confined by the first and third quartile and the whiskers extend to 1.5 times the interquartile distance. Points falling outside the whiskers are considered outliers and plotted as dots.

**Fig. 3** Limitation of photosynthesis ( $A$ ) after the increase in light intensity from 100 to 1000  $\mu\text{mol m}^{-2}\text{s}^{-1}$ . (A) Time to reach 95 % of the steady-state  $A$  for five different banana genotypes. (B) Percentage limitation of  $A$  after the increase in light intensity. Different letters indicate significant differences between genotypes (post hoc Tukey HSD test,  $P < 0.05$ ;  $n = 7-8$ ;  $A > B$ ). The bold middle line in boxplots represents the median. The box is confined by the first and third quartile and the whiskers extend to 1.5 times the interquartile distance. Points falling outside the whiskers are considered outliers and plotted as dots.

**Fig. 4** Relation between abaxial stomatal density and the time constant describing the speed of stomatal conductance increase ( $K_i$ ) after the light intensity increase from 100 to 1000  $\mu\text{mol m}^{-2}\text{s}^{-1}$ . There was no significant correlation (Pearson's correlation test), caused by the outlying genotype Cachaco. Points and error bars represent mean  $\pm$  SE ( $n = 7-8$ ).

**Fig. 5** Gravimetric transpiration rate analysis of genotypes Cachaco and Mbwarzirume at dawn after a step increase in light intensity from 0 to  $120 \mu\text{mol m}^{-2} \text{s}^{-1}$ . (A) A breakpoint was identified in whole-plant transpiration after the step increase in light intensity. The timing of the breakpoint in transpiration after dawn differed significantly between the genotype Cachaco and Mbwarzirume ( $n = 24$ ,  $P < 0.01$ , linear mixed-effects model with plant-specific and date-specific random effect). (B) Transpiration rate after dawn increased faster in Mbwarzirume compared to Cachaco. Before dawn transpiration rates did not differ significantly. Similarly transpiration rates do not differ significantly after 90 minutes (24 datapoints per per time range for both Cachaco and Mbwarzirume, \* for  $P < 0.05$ , \*\* for  $P < 0.01$ , linear mixed-effects model with plant-specific and date-specific random effect). Grey areas indicate the time before dawn .. The bold middle line in boxplots represents the median The box is confined by the first and third quartile and the whiskers extend to 1.5 times the interquartile distance.

**Fig. 6** Morning response of stomatal conductance ( $g_s$ ) and photosynthesis (A) of the genotypes Cachaco and Mbwarzirume. (A) Time course of the  $g_s$  response to a gradual increase in light intensity at dawn (black line). Data are the mean  $\pm$  SE ( $n = 4$ ). (B) The time constant of  $g_s$  increase ( $K_i$ ) during the first 90 min after dawn was significantly higher in Cachaco. (C) The difference in  $g_s$  rapidity at dawn did not result in different A between both genotypes. Data represents the mean  $\pm$  SE ( $n = 4$ ). (D) The mean intrinsic water use efficiency ( $i\text{WUE}$ ) during the first 90 min after dawn was significantly higher in Cachaco compared to Mbwarzirume. The grey area indicates the time before dawn. PPFD, Photosynthetic Photon Flux Density. (Student's  $t$  test, \*for  $P < 0.05$ , \*\* for  $P < 0.01$ ).

**Fig. 7** Mean diurnal time course of measured photosynthesis ( $A_{\text{measured}}$ ) and maximal photosynthesis ( $A_{\text{max}}$ , black line) under fluctuating light conditions for Mbwarzirume and Cachaco. The  $A_{\text{max}}$  at each light intensity was determined by a modelled light response curve. The nonrectangular hyperbola-based model of Prioul & Chartier (1997) was optimized as described by Lobo et al. (2013). Grey areas indicate times of darkness, red areas indicate the difference between maximal A and measured A. Data are the mean  $\pm$  SE ( $n = 4$ ).

**Fig. 8** Diurnal time course of gas exchange parameters of the genotypes Mbwarzirume and Cachaco under fluctuating light conditions. (A) stomatal conductance ( $g_s$ ), (B) photosynthesis (A) and (C) intrinsic water use efficiency ( $i\text{WUE}$ ) The light intensity fluctuated throughout the

day (black line). The significance of the time constant of  $g_s$  increase or decrease ( $K$ ) and the maximal slope of  $g_s$  increase or decrease ( $Sl_{max}$ ) is shown (Student's  $t$  test, \*for  $P < 0.05$  and \*\* for  $P < 0.01$  for faster  $g_s$  rapidity in Mbwarzirume compared to Cachaco). Throughout the day,  $g_s$  kinetics were faster for the genotype Mbwarzirume compared to Cachaco, but differences were dependent on the target light intensity, the magnitude of change, the  $g_s$  prior to the intensity change and the time of the day. Grey areas indicate times of darkness. Green areas indicate the analyzed time frame of the  $g_s$  rapidity response. Blue areas indicate time points with significant differences in  $A$  or  $iWUE$  between both genotypes (Student's  $t$  test,  $P < 0.05$ ). PPF, Photosynthetic Photon Flux Density. Data are the mean  $\pm$  SE ( $n = 4$ ).

**Fig. 9** Average diurnal gas exchange parameters of the genotypes Mbwarzirume and Cachaco under fluctuating light conditions illustrated in Fig. 8. (A) stomatal conductance ( $g_s$ ), (B) photosynthesis ( $A$ ) and (C) intrinsic water use efficiency ( $iWUE$ ). (D) The percentage limitation of  $A$  during the afternoon ( $> 6$  hours after light onset). (Student's  $t$  test, \* for  $P < 0.05$ ,  $n = 4$ ).

## Literature Cited

- Acevedo-Siaca LG, Coe R, Wang Y, Kromdijk J, Quick WP, Long SP** (2020) Variation in photosynthetic induction between rice accessions and its potential for improving productivity. *New Phytol* **227**: 1097–1108
- Assmann SM, Shimazaki KI** (1999) The multisensory guard cell. Stomatal responses to blue light and abscisic acid. *Plant Physiol* **119**: 809–815
- Aubert B, Catsky J** (1970) The onset of photosynthetic CO<sub>2</sub> influx in banana leaf segments as related to stomatal diffusion resistance at different air humidities. *Photosynthetica* **4**: 254–256
- Barradas VL, Jones HG** (1996) Responses of CO<sub>2</sub> assimilation to changes in irradiance: laboratory and field data and a model for beans (*Phaseolus vulgaris* L.). *J Exp Bot* **47**: 639–645
- Brun W** (1961) Photosynthesis & transpiration from upper & lower surfaces of intact banana leaves. *Plant Physiol* **36**: 399–405
- Chaves MM, Costa JM, Zarrouk O, Pinheiro C, Lopes CM, Pereira JS** (2016) Controlling stomatal aperture in semi-arid regions—The dilemma of saving water or being cool? *Plant Sci* **251**: 54–64
- Deans RM, Brodribb TJ, Busch FA, Farquhar GD** (2019a) Plant water-use strategy mediates stomatal effects on the light induction of photosynthesis. *New Phytol* **222**: 382–395
- Deans RM, Farquhar GD, Busch FA** (2019b) Estimating stomatal and biochemical limitations during photosynthetic induction. *Plant Cell Environ* **42**: 3227–3240
- Delorge I, Janiak M, Carpentier S, Van Dijck P** (2014) Fine tuning of trehalose biosynthesis and hydrolysis as novel tools for the generation of abiotic stress tolerant plants. *Front Plant Sci*. doi: 10.3389/fpls.2014.00147
- Drake PL, Froend RH, Franks PJ** (2012) Smaller , faster stomata : scaling of stomatal size , rate of response , and stomatal conductance. *J Exp Bot* **64**: 495–505
- Durand M, Brendel O, Buré C, Le Thiec D** (2020) Changes in irradiance and vapour pressure deficit under drought induce distinct stomatal dynamics between glasshouse and field-grown poplars. *New Phytol* **227**: 392–406
- Eyland D, Breton C, Sardos J, Kallow S, Panis B, Swennen R, Paofa J, Tardieu F, Welcker C, Janssens SB, et al** (2021) Filling the gaps in gene banks: Collecting, characterizing, and phenotyping wild banana relatives of Papua New Guinea. *Crop Sci* **61**: 137–149
- Faralli M, Cockram J, Ober E, Wall S, Galle A, Rie J Van, Raines C, Lawson T, Casson SA, Christian C, et al** (2019a) Genotypic, developmental and environmental effects on the rapidity of gs in wheat : impacts on carbon gain and water-use efficiency. *Front Plant Sci* **10**: 1–13
- Faralli M, Matthews J, Lawson T** (2019b) Exploiting natural variation and genetic manipulation of stomatal conductance for crop improvement. *Curr Opin Plant Biol* **49**: 1–7



- Farquhar GD, Caemmerer S, Berry JA** (1980) A biochemical model of photosynthetic CO<sub>2</sub> assimilation in leaves of C<sub>3</sub> species. *Planta* **149**: 78–90
- Farquhar GD, Sharkey TD** (1982) Stomatal conductance and photosynthesis. *Annu Rev Plant Physiol* **33**: 317–345
- Fischer RA, Rees D, Sayre KD, Lu ZM, Condon AG, Larque Saavedra A** (1998) Wheat yield progress associated with higher stomatal conductance and photosynthetic rate, and cooler canopies. *Crop Sci* **38**: 1467–1475
- Franks PJ** (2006) Higher rates of leaf gas exchange are associated with higher leaf hydrodynamic pressure gradients. *Plant, Cell Environ* **29**: 584–592
- Franks PJ, Farquhar GD** (2007) The mechanical diversity of stomata and its significance in gas-exchange control. *Plant Physiol* **143**: 78–87
- Gosa SC, Lupo Y, Moshelion M** (2019) Quantitative and comparative analysis of whole-plant performance for functional physiological traits phenotyping: New tools to support pre-breeding and plant stress physiology studies. *Plant Sci* **282**: 49–59
- Grassi G, Magnani F** (2005) Stomatal, mesophyll conductance and biochemical limitations to photosynthesis as affected by drought and leaf ontogeny in ash and oak trees. *Plant, Cell Environ* **28**: 834–849
- Haydon MJ, Mielczarek O, Robertson FC, Hubbard KE, Webb AAR** (2013) Photosynthetic entrainment of the *Arabidopsis thaliana* circadian clock. *Nature* **502**: 689–692
- Hermida-Carrera C, Kapralov M V., Galmés J** (2016) Rubisco catalytic properties and temperature response in crops. *Plant Physiol* **171**: 2549–2561
- Hetherington AM, Woodward FI** (2003) The role of stomata in sensing and driving environmental change. *Nature* **424**: 901–908
- Janssens SB, Vandeloock F, De Langhe E, Verstraete B, Smets E, Vandenhouwe I, Swennen R** (2016) Evolutionary dynamics and biogeography of Musaceae reveal a correlation between the diversification of the banana family and the geological and climatic history of Southeast Asia. *New Phytol* **210**: 1453–1465
- Jones H** (1998) Stomatal control of photosynthesis and transpiration. *J Exp Bot* **49**: 387–398
- Jones HG** (1985) Partitioning stomatal and non-stomatal limitations to photosynthesis. *Plant, Cell Environ* **8**: 95–104
- Kaiser E, Morales A, Harbinson J, Heuvelink E, Prinzenberg AE, Marcelis LFM** (2016) Metabolic and diffusional limitations of photosynthesis in fluctuating irradiance in *Arabidopsis thaliana*. *Sci Rep* **6**: 1–13
- Kimura H, Hashimoto-Sugimoto M, Iba K, Terashima I, Yamori W** (2020) Improved stomatal opening enhances photosynthetic rate and biomass production in fluctuating light. *J Exp Bot* **71**: 2339–2350
- Lawson T, Blatt MR** (2014) Stomatal size, speed, and responsiveness impact on photosynthesis and water use efficiency. *Plant Physiol* **164**: 1556–1570

- Lawson T, Morison JIL** (2004) Stomatal function and physiology. *Evol. Plant Physiol.* Elsevier, pp 217–242
- Lobo F de A, de Barros MP, Dalmagro HJ, Dalmolin ÂC, Pereira WE, de Souza ÉC, Vourlitis GL, Rodríguez Ortiz CE** (2013) Fitting net photosynthetic light-response curves with Microsoft Excel - a critical look at the models. *Photosynthetica* **51**: 445–456
- Matthews JSA, Vialet-Chabrand SRM, Lawson T** (2017) Diurnal variation in gas exchange: the balance between carbon fixation and water loss. *Plant Physiol* **174**: 614–623
- McAusland L, Vialet-Chabrand S, Davey P, Baker NR, Brendel O, Lawson T** (2016) Effects of kinetics of light-induced stomatal responses on photosynthesis and water-use efficiency. *New Phytol* **211**: 1209–1220
- Mencuccini M, Mambelli S, Comstock J** (2000) Stomatal responsiveness to leaf water status in common bean (*Phaseolus vulgaris* L.) is a function of time of day. *Plant Cell Environ* **23**: 1109–1118
- Morales A, Kaiser E** (2020) Photosynthetic acclimation to fluctuating irradiance in plants. *Front Plant Sci* **11**: 1–12
- Mott KA, Woodrow IE** (2000) Modelling the role of Rubisco activase in limiting non-steady-state photosynthesis. *J Exp Bot* **51**: 399–406
- Outlaw WHJ** (2003) Integration of cellular and physiological functions of guard cells. *CRC Crit Rev Plant Sci* **22**: 503–529
- Paine CET, Marthews TR, Vogt DR, Purves D, Rees M, Hector A, Turnbull LA** (2012) How to fit nonlinear plant growth models and calculate growth rates: an update for ecologists. *Methods Ecol Evol* **3**: 245–256
- Papanatsiou M, Petersen J, Henderson L, Wang Y, Christie JM, Blatt MR** (2019) Optogenetic manipulation of stomatal kinetics improves carbon assimilation, water use, and growth. *Science* (80- ) **363**: 1456–1459
- Pearcy RW** (1990) Sunflecks and photosynthesis in plant canopies. *Annu Rev Plant Physiol Plant Mol Biol* **41**: 421–453
- Perrier X, De Langhe E, Donohue M, Lentfer C, Vrydaghs L, Bakry F, Carreel F, Hippolyte I, Horry J-P, Jenny C, et al** (2011) Multidisciplinary perspectives on banana (*Musa* spp.) domestication. *PNAS* **108**: 11311–11318
- Prioul JL, Chartier P** (1977) Partitioning of transfer and carboxylation components of intracellular resistance to photosynthetic CO<sub>2</sub> fixation: A critical analysis of the methods used. *Ann Bot* **41**: 789–800
- Qu M, Hamdani S, Li W, Wang S, Tang J, Chen Z, Song Q, Li M, Zhao H, Chang T, et al** (2016) Rapid stomatal response to fluctuating light: an under-explored mechanism to improve drought tolerance in rice. *Funct Plant Biol* **43**: 727
- Raven JA** (2014) Speedy small stomata? *J Exp Bot* **65**: 1415–1424
- Resco de Dios V, Gessler A** (2018) Circadian regulation of photosynthesis and transpiration

from genes to ecosystems. *Environ Exp Bot* **152**: 37–48

**Rudall PJ, Chen ED, Cullen E** (2017) Evolution and development of monocot stomata. *Am J Bot* **104**: 1122–1141

**Sakoda K, Yamori W, Shimada T, Sugano SS, Hara-Nishimura I, Tanaka Y** (2020) Higher stomatal density improves photosynthetic induction and biomass production in *Arabidopsis* under fluctuating light. *Front Plant Sci*. doi: 10.3389/fpls.2020.589603

**Savitzky A, Golay MJE** (1964) Smoothing and Differentiation of Data by Simplified Least Squares Procedures. *Anal Chem* **36**: 1627–1639

**Slattery RA, Walker BJ, Weber APM, Ort DR** (2018) The impacts of fluctuating light on crop performance. *Plant Physiol* **176**: 990–1003

**Soleh MA, Tanaka Y, Kim SY, Huber SC, Sakoda K, Shiraiwa T** (2017) Identification of large variation in the photosynthetic induction response among 37 soybean [*Glycine max* (L.) Merr.] genotypes that is not correlated with steady-state photosynthetic capacity. *Photosynth Res* **131**: 305–315

**De Souza AP, Wang Y, Orr DJ, Carmo-Silva E, Long SP** (2020) Photosynthesis across African cassava germplasm is limited by Rubisco and mesophyll conductance at steady state, but by stomatal conductance in fluctuating light. *New Phytol* **225**: 2498–2512

**Taylor SH, Long SP** (2017) Slow induction of photosynthesis on shade to sun transitions in wheat may cost at least 21% of productivity. *Philos Trans R Soc B Biol Sci*. doi: 10.1098/rstb.2016.0543

**Turner DW, Thomas DS** (1998) Measurements of plant and soil water status and their association with leaf gas exchange in banana (*Musa* spp.): A laticiferous plant. *Sci Hortic (Amsterdam)* **77**: 177–193

**Urban O, Šprtová M, Košvancová M, Tomášková I, Lichtenthaler HK, Marek M V.** (2008) Comparison of photosynthetic induction and transient limitations during the induction phase in young and mature leaves from three poplar clones. *Tree Physiol* **28**: 1189–1197

**Vialet-Chabrand S, Dreyer E, Brendel O** (2013) Performance of a new dynamic model for predicting diurnal time courses of stomatal conductance at the leaf level. *Plant, Cell Environ* **36**: 1529–1546

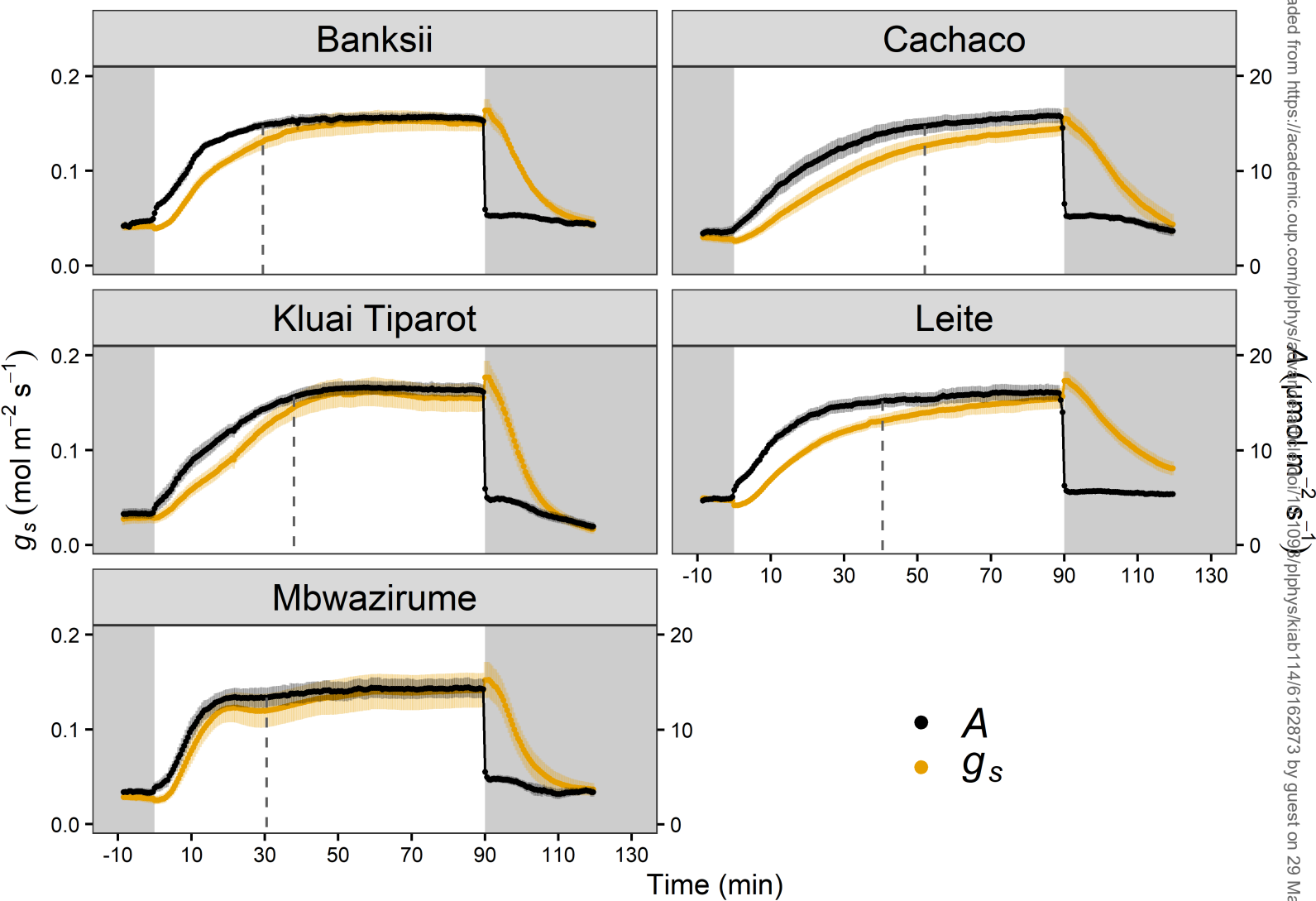
**Vialet-Chabrand SRM, Matthews JSA, McAusland L, Blatt MR, Griffiths H, Lawson T** (2017) Temporal Dynamics of Stomatal Behavior: Modeling and Implications for Photosynthesis and Water Use. *Plant Physiol* **174**: 603–613

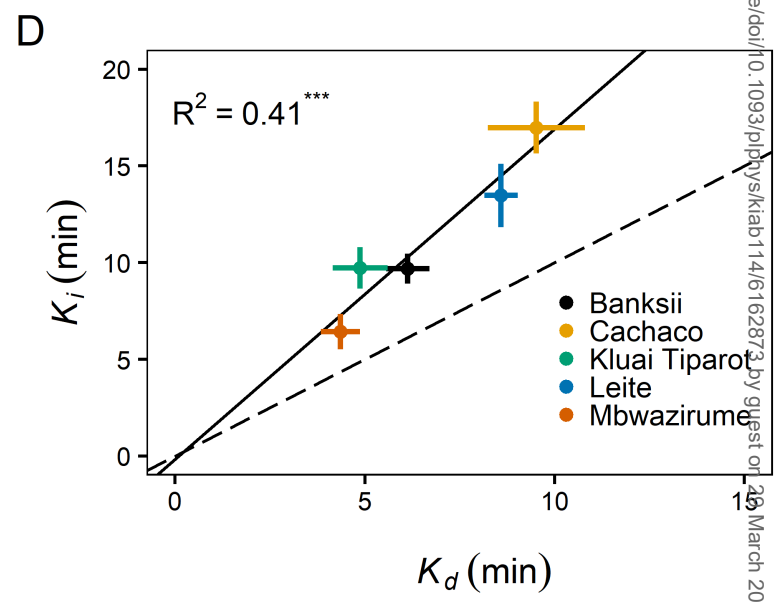
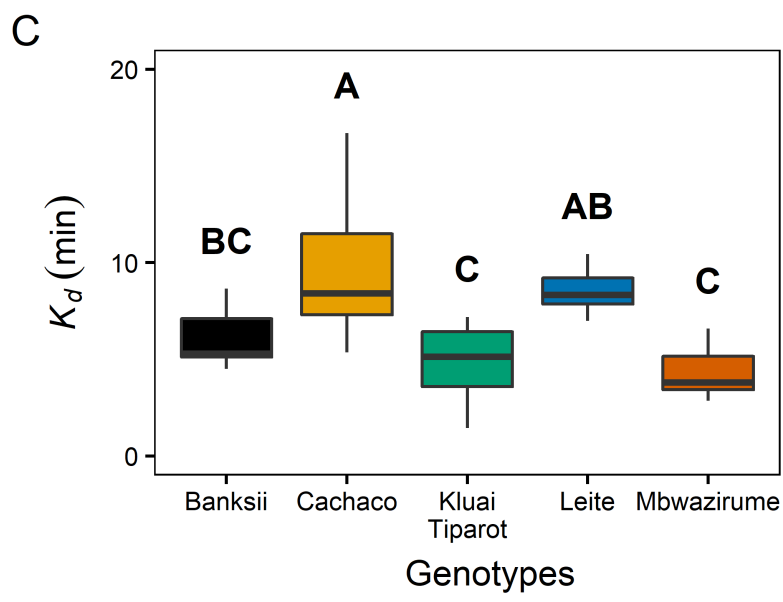
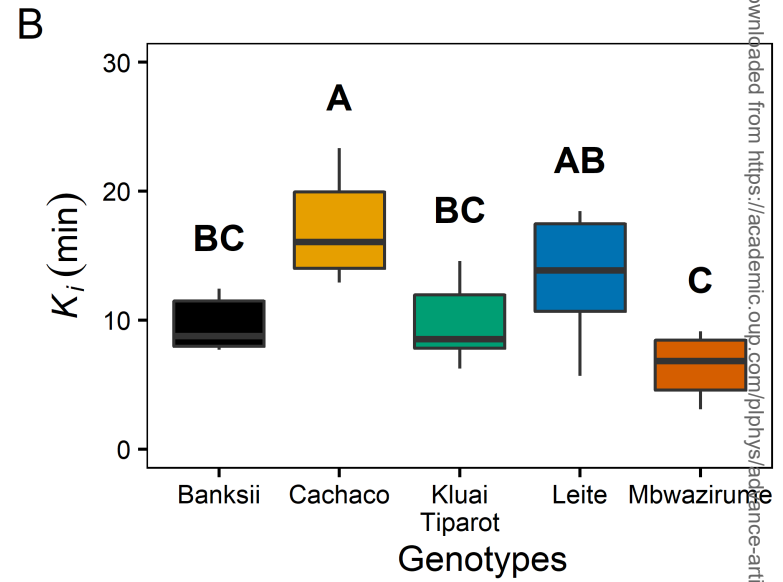
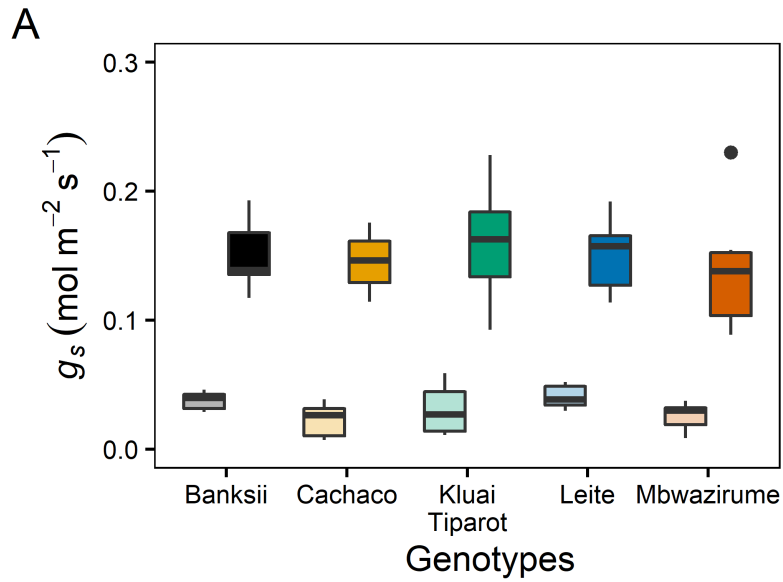
**Vico G, Manzoni S, Palmroth S, Katul G** (2011) Effects of stomatal delays on the economics of leaf gas exchange under intermittent light regimes. *New Phytol* **192**: 640–652

**Wachendorf M, Küppers M** (2017) The effect of initial stomatal opening on the dynamics of biochemical and overall photosynthetic induction. *Trees - Struct Funct* **31**: 981–995

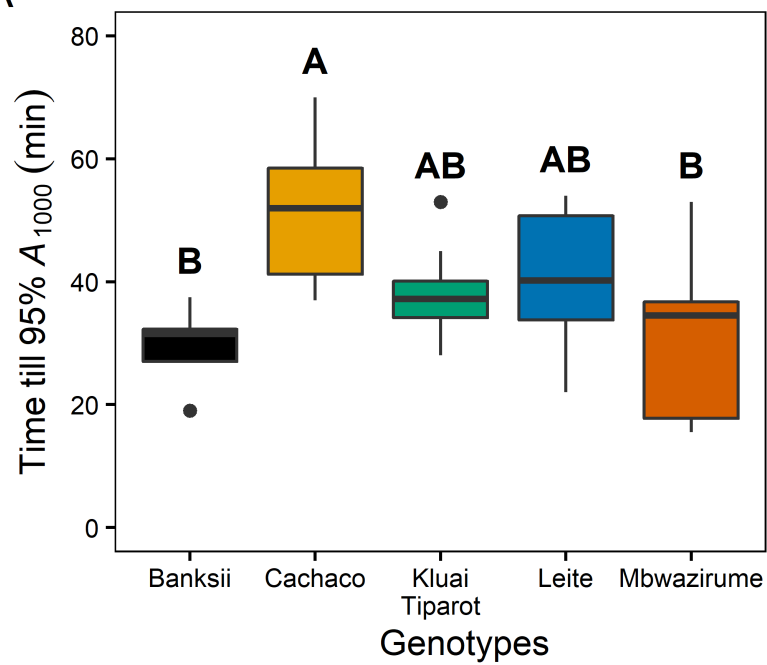
**Way DA, Percy RW** (2012) Sunflecks in trees and forests: From photosynthetic physiology to global change biology. *Tree Physiol* **32**: 1066–1081

- van Wesemael J, Kissel E, Eyland D, Lawson T, Swennen R, Carpentier S** (2019) Using growth and transpiration phenotyping under controlled conditions to select water efficient banana genotypes. *Front Plant Sci* **10**: 1–14
- Weyers JDB, Johansen LG** (1985) Accurate estimation of stomatal aperture from silicone rubber impressions. *New Phytol* **101**: 109–115
- Wilson KB, Baldocchi DD, Hanson PJ** (2000) Quantifying stomatal and non-stomatal limitations to carbon assimilation resulting from leaf aging and drought in mature deciduous tree species. *Tree Physiol* **20**: 787–797
- Yamori W, Kusumi K, Iba K, Terashima I** (2020) Increased stomatal conductance induces rapid changes to photosynthetic rate in response to naturally fluctuating light conditions in rice. *Plant Cell Environ* **43**: 1230–1240

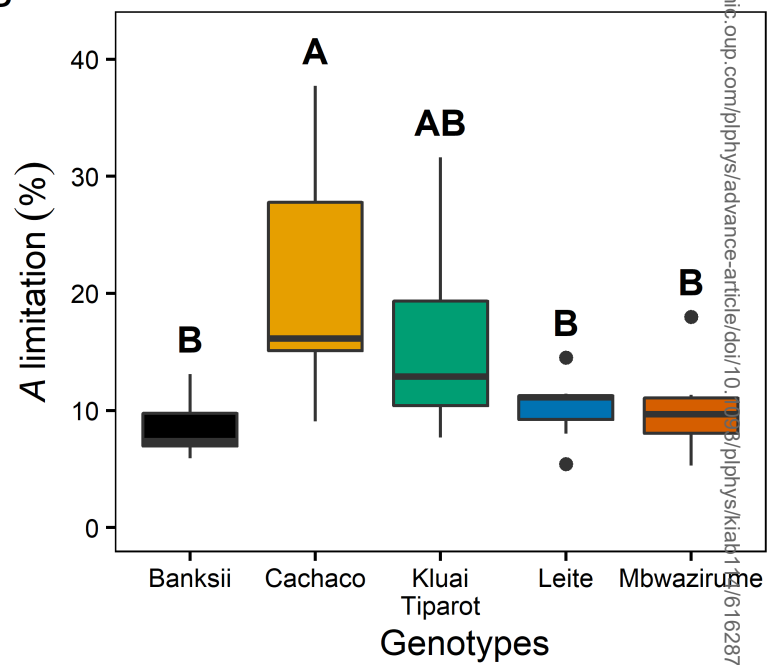


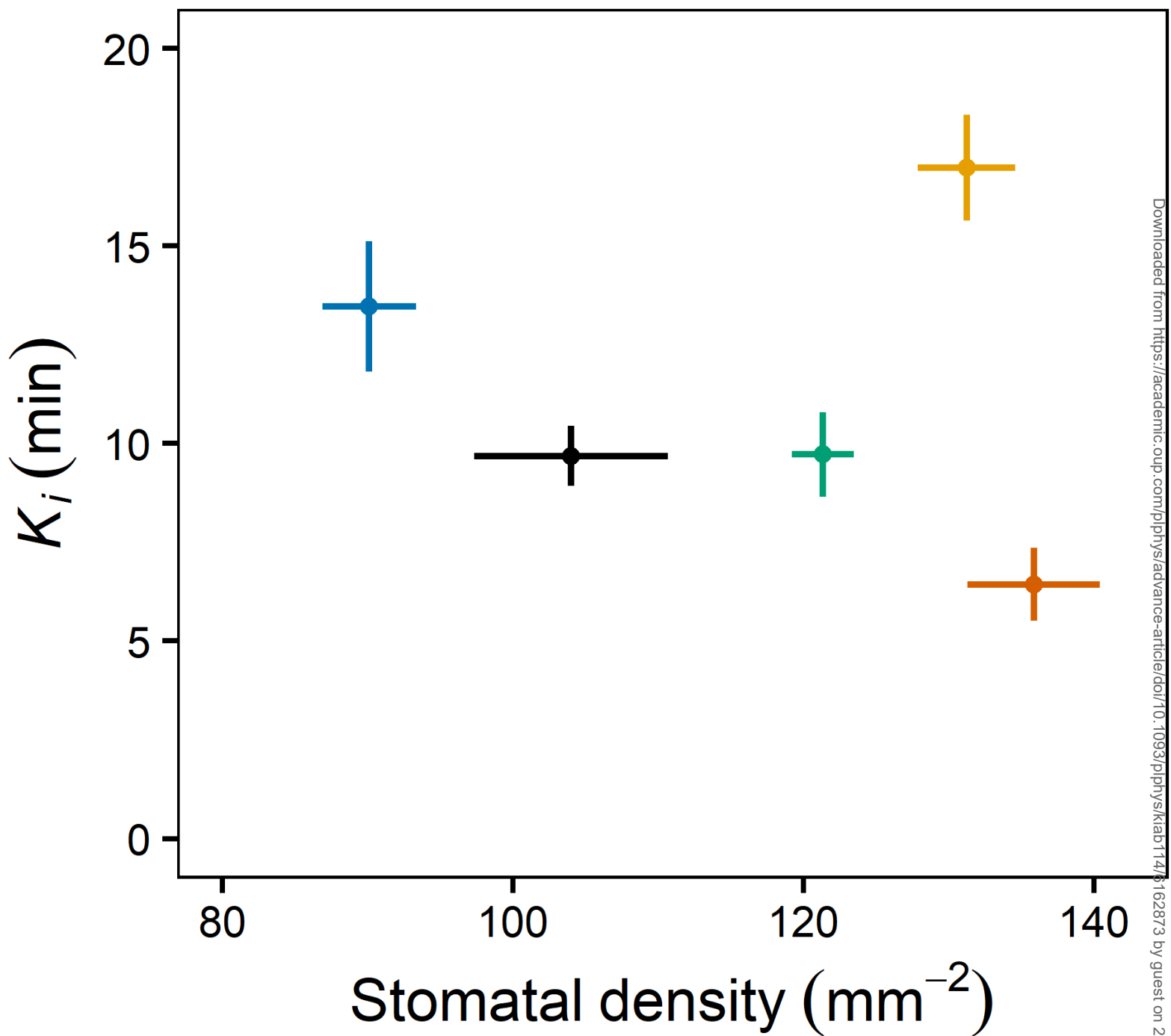


**A**



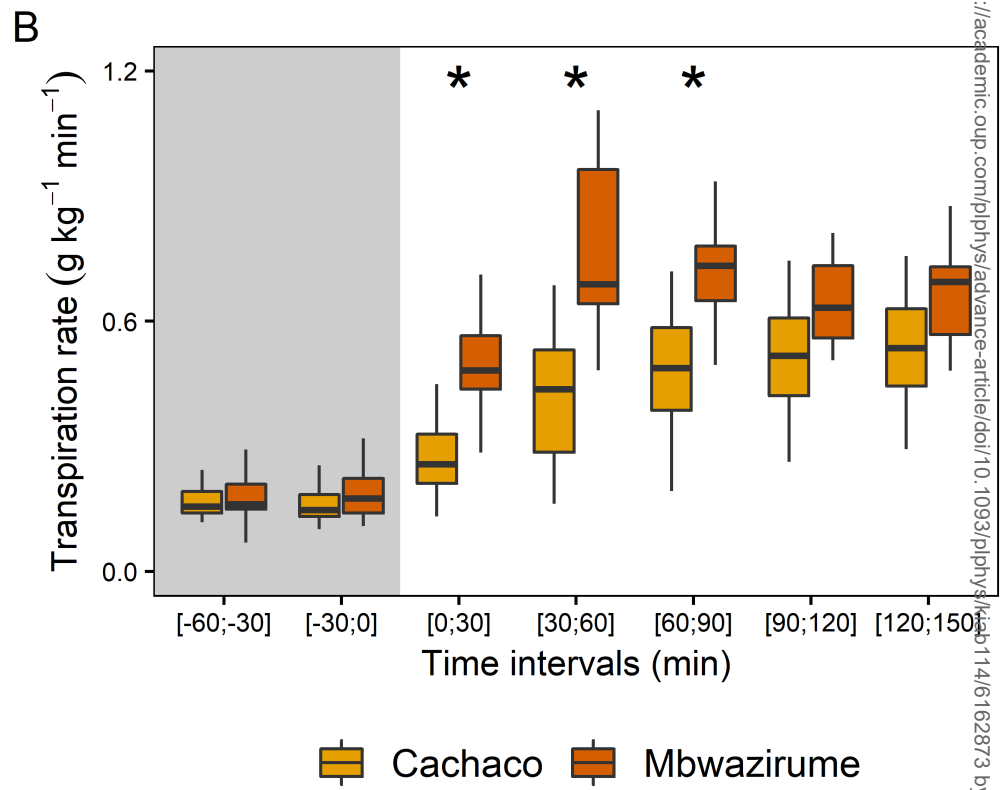
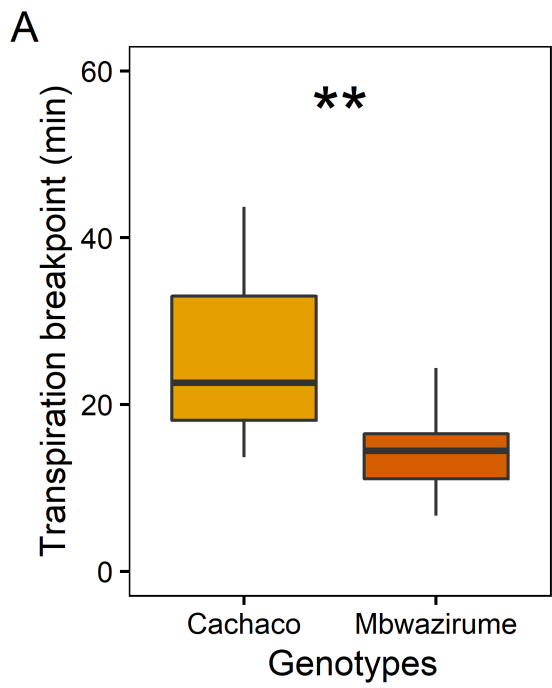
**B**

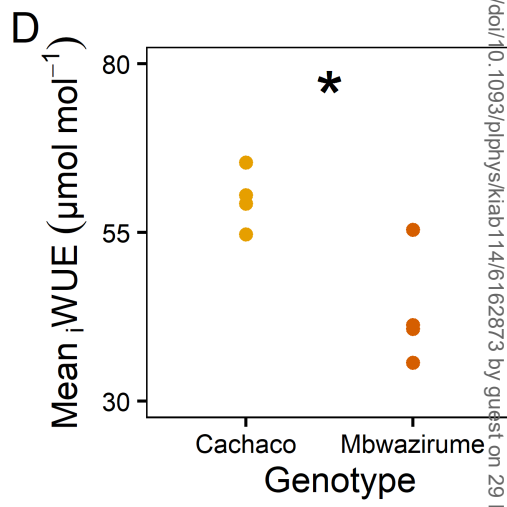
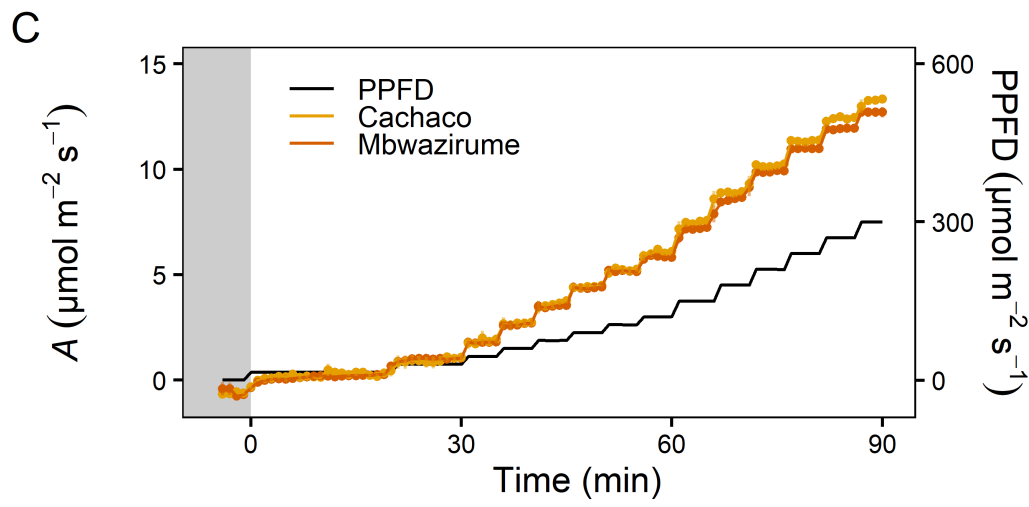
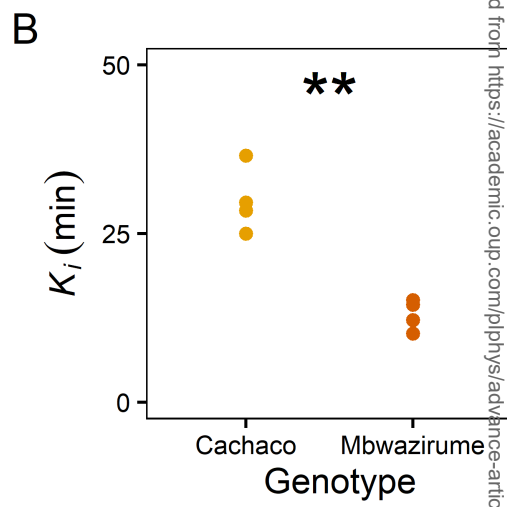
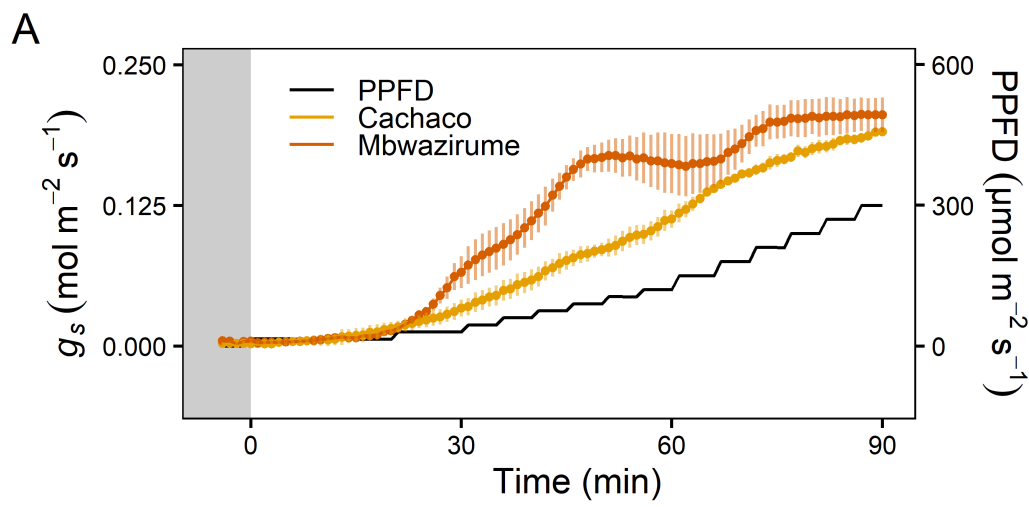


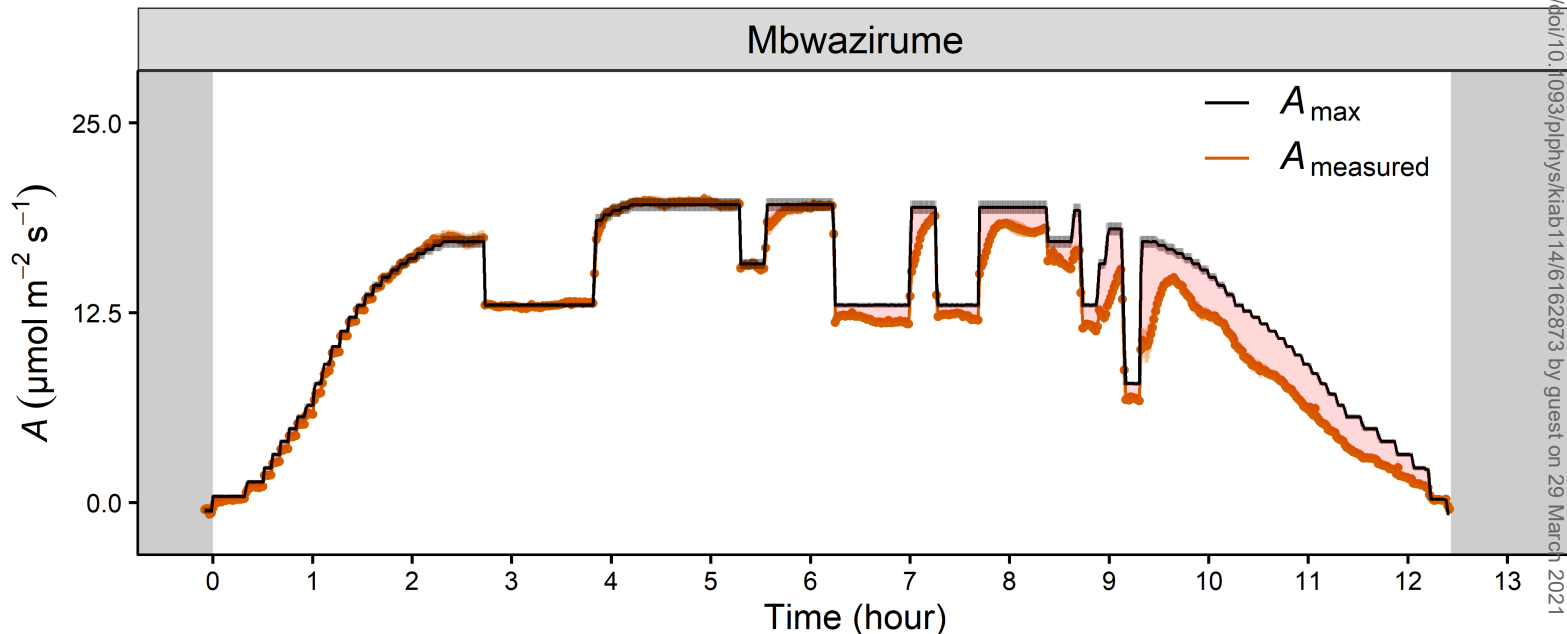
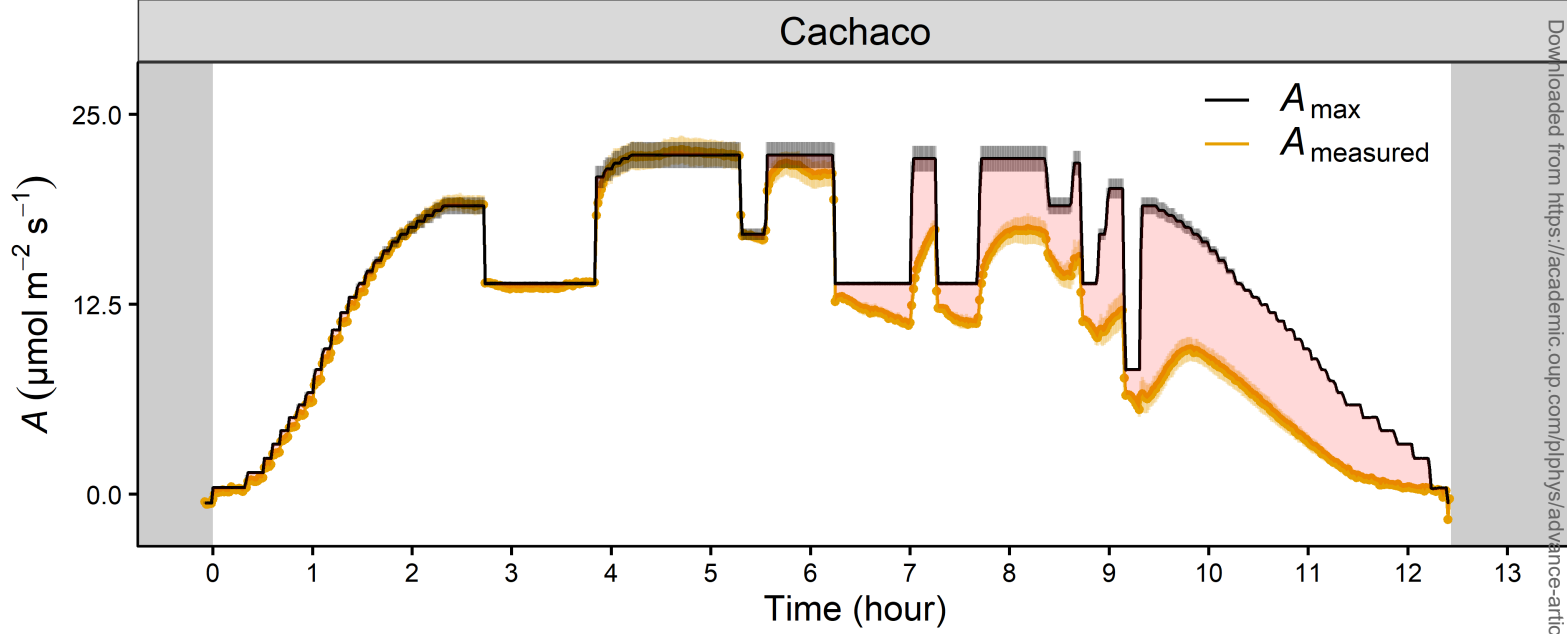


- Banksii
- Kluai Tiparot
- Mbwazirume
- Cachaco
- Leite

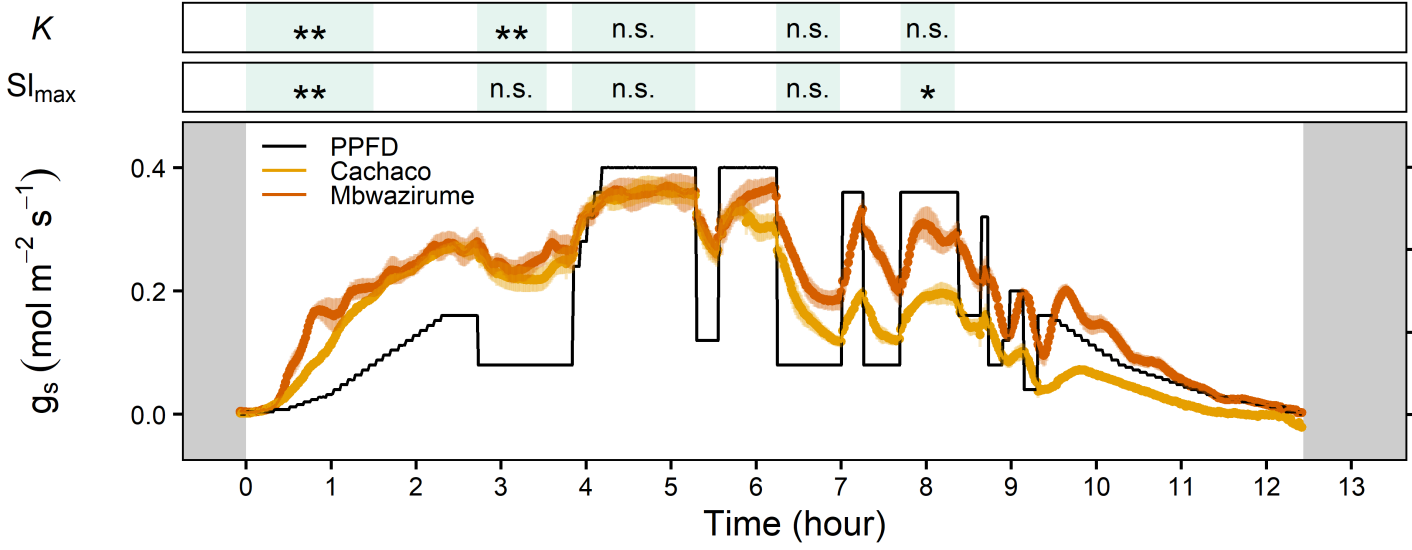




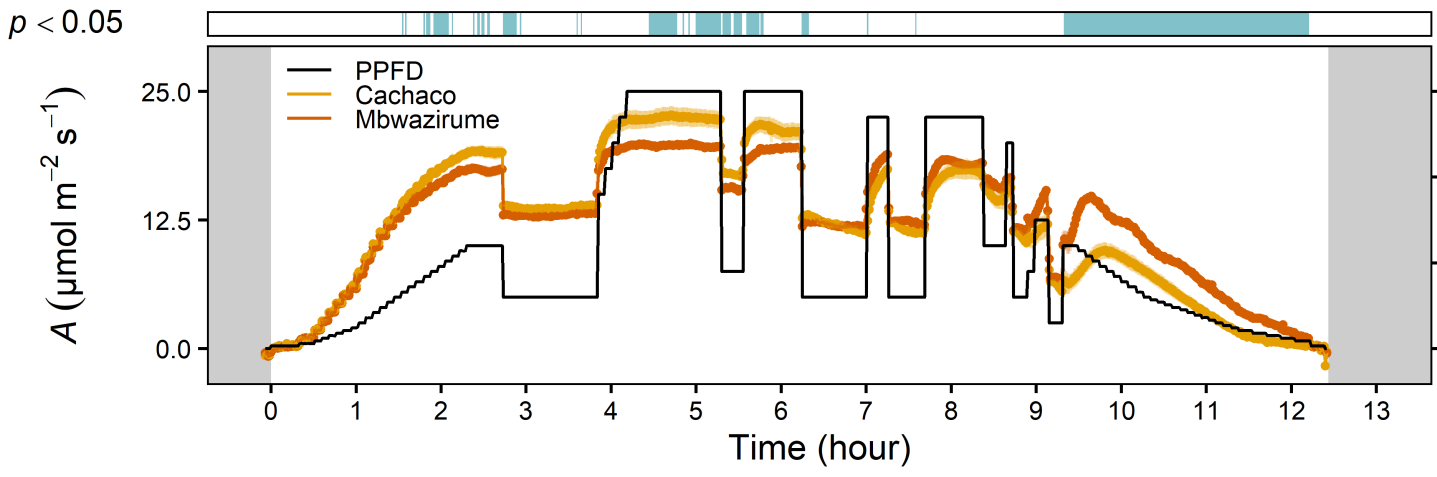




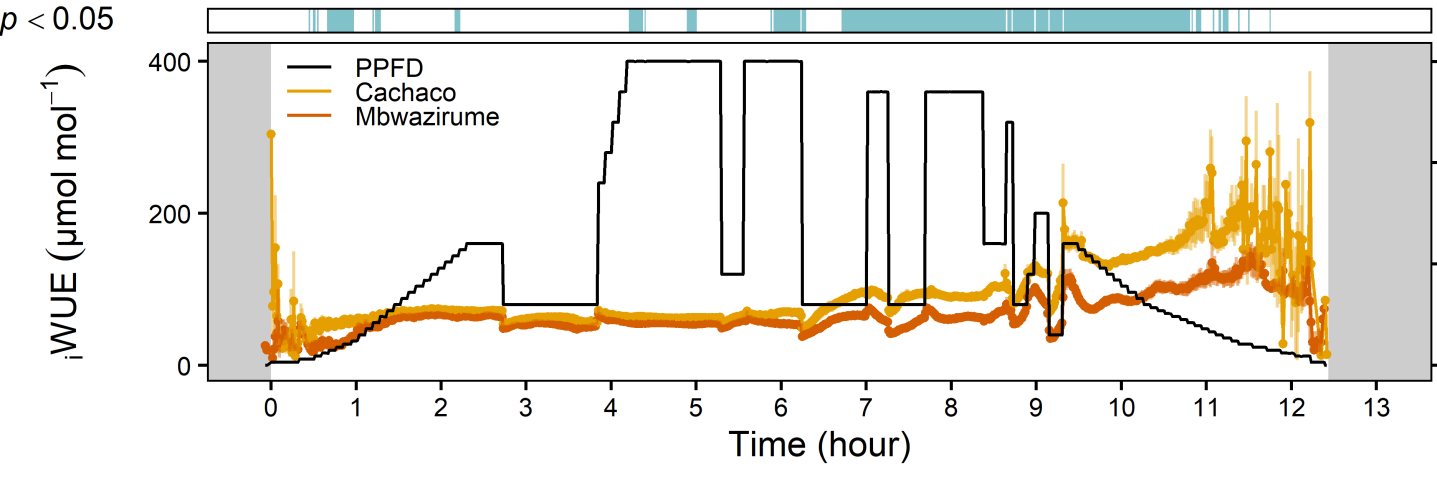
A

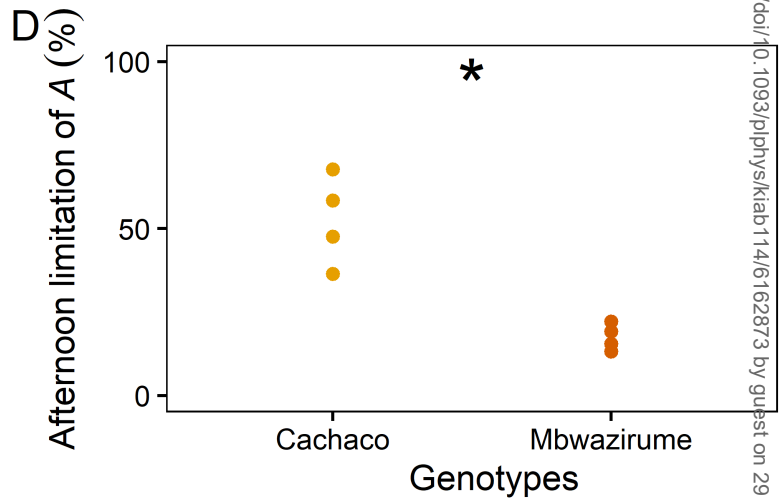
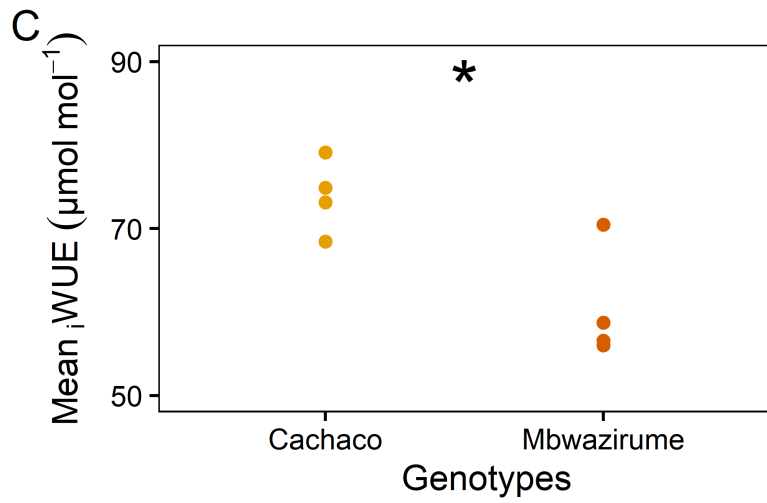
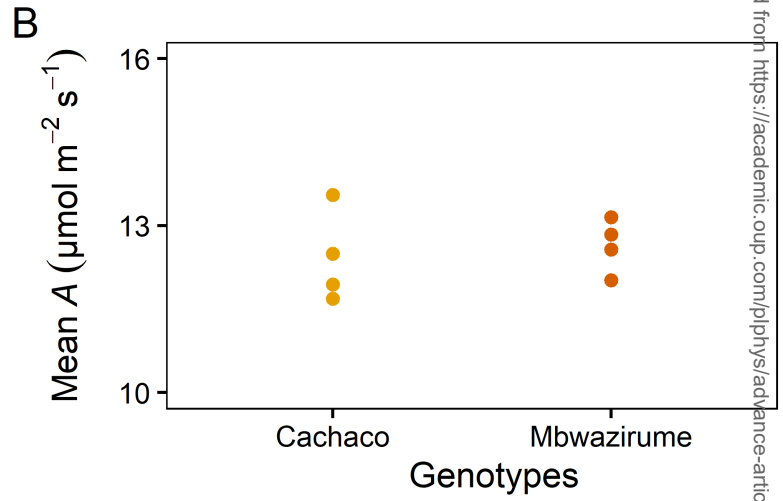
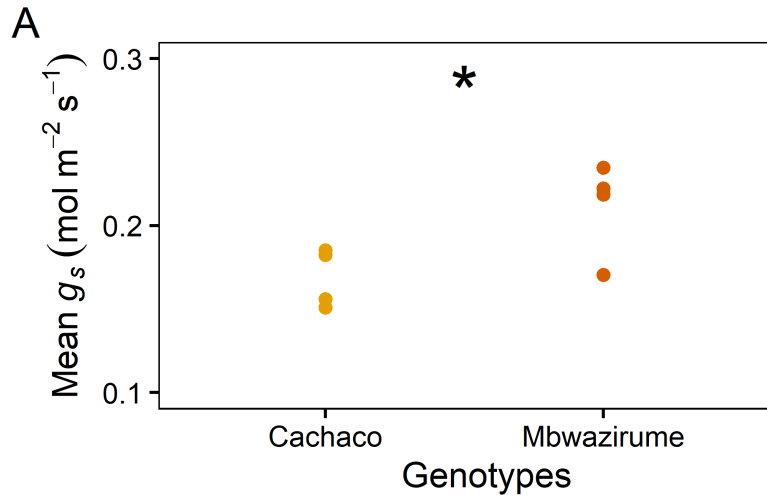


B



C





## Parsed Citations

Acevedo-Siaca LG, Coe R, Wang Y, Kromdijk J, Quick WP, Long SP (2020) Variation in photosynthetic induction between rice accessions and its potential for improving productivity. *New Phytol* 227: 1097–1108

Google Scholar: [Author Only](#) [Title Only](#) [Author and Title](#)

Assmann SM, Shimazaki KI (1999) The multisensory guard cell. Stomatal responses to blue light and abscisic acid. *Plant Physiol* 119: 809–815

Google Scholar: [Author Only](#) [Title Only](#) [Author and Title](#)

Aubert B, Catsky J (1970) The onset of photosynthetic CO<sub>2</sub> influx in banana leaf segments as related to stomatal diffusion resistance at different air humidities. *Photosynthetica* 4: 254–256

Google Scholar: [Author Only](#) [Title Only](#) [Author and Title](#)

Barradas VL, Jones HG (1996) Responses of CO<sub>2</sub> assimilation to changes in irradiance: laboratory and field data and a model for beans (*Phaseolus vulgaris* L.). *J Exp Bot* 47: 639–645

Google Scholar: [Author Only](#) [Title Only](#) [Author and Title](#)

Brun W (1961) Photosynthesis & transpiration from upper & lower surfaces of intact banana leaves. *Plant Physiol* 36: 399–405

Google Scholar: [Author Only](#) [Title Only](#) [Author and Title](#)

Chaves MM, Costa JM, Zarrouk O, Pinheiro C, Lopes CM, Pereira JS (2016) Controlling stomatal aperture in semi-arid regions—The dilemma of saving water or being cool? *Plant Sci* 251: 54–64

Deans RM, Brodribb TJ, Busch FA, Farquhar GD (2019a) Plant water-use strategy mediates stomatal effects on the light induction of photosynthesis. *New Phytol* 222: 382–395

Google Scholar: [Author Only](#) [Title Only](#) [Author and Title](#)

Deans RM, Farquhar GD, Busch FA (2019b) Estimating stomatal and biochemical limitations during photosynthetic induction. *Plant Cell Environ* 42: 3227–3240

Google Scholar: [Author Only](#) [Title Only](#) [Author and Title](#)

Delorge I, Janiak M, Carpentier S, Van Dijk P (2014) Fine tuning of trehalose biosynthesis and hydrolysis as novel tools for the generation of abiotic stress tolerant plants. *Front Plant Sci*. doi: 10.3389/fpls.2014.00147

Google Scholar: [Author Only](#) [Title Only](#) [Author and Title](#)

Drake PL, Froend RH, Franks PJ (2012) Smaller, faster stomata: scaling of stomatal size, rate of response, and stomatal conductance. *J Exp Bot* 64: 495–505

Google Scholar: [Author Only](#) [Title Only](#) [Author and Title](#)

Durand M, Brendel O, Buré C, Le Thiec D (2020) Changes in irradiance and vapour pressure deficit under drought induce distinct stomatal dynamics between glasshouse and field-grown poplars. *New Phytol* 227: 392–406

Google Scholar: [Author Only](#) [Title Only](#) [Author and Title](#)

Eyland D, Breton C, Sardos J, Kallow S, Panis B, Swennen R, Paofa J, Tardieu F, Welcker C, Janssens SB, et al (2021) Filling the gaps in gene banks: Collecting, characterizing, and phenotyping wild banana relatives of Papua New Guinea. *Crop Sci* 61: 137–149

Google Scholar: [Author Only](#) [Title Only](#) [Author and Title](#)

Faralli M, Cockram J, Ober E, Wall S, Galle A, Rie J Van, Raines C, Lawson T, Casson SA, Christian C, et al (2019a) Genotypic, developmental and environmental effects on the rapidity of g<sub>s</sub> in wheat: impacts on carbon gain and water-use efficiency. *Front Plant Sci* 10: 1–13

Google Scholar: [Author Only](#) [Title Only](#) [Author and Title](#)

Faralli M, Matthews J, Lawson T (2019b) Exploiting natural variation and genetic manipulation of stomatal conductance for crop improvement. *Curr Opin Plant Biol* 49: 1–7

Google Scholar: [Author Only](#) [Title Only](#) [Author and Title](#)

Farquhar GD, Caemmerer S, Berry JA (1980) A biochemical model of photosynthetic CO<sub>2</sub> assimilation in leaves of C<sub>3</sub> species. *Planta* 149: 78–90–90

Google Scholar: [Author Only](#) [Title Only](#) [Author and Title](#)

Farquhar GD, Sharkey TD (1982) Stomatal conductance and photosynthesis. *Annu Rev Plant Physiol* 33: 317–345

Google Scholar: [Author Only](#) [Title Only](#) [Author and Title](#)

Fischer RA, Rees D, Sayre KD, Lu ZM, Condon AG, Larque Saavedra A (1998) Wheat yield progress associated with higher stomatal conductance and photosynthetic rate, and cooler canopies. *Crop Sci* 38: 1467–1475

Google Scholar: [Author Only](#) [Title Only](#) [Author and Title](#)

Franks PJ (2006) Higher rates of leaf gas exchange are associated with higher leaf hydrodynamic pressure gradients. *Plant, Cell Environ* 29: 584–592

Google Scholar: [Author Only](#) [Title Only](#) [Author and Title](#)

Franks PJ, Farquhar GD (2007) The mechanical diversity of stomata and its significance in gas-exchange control. *Plant Physiol* 143: 78–

- Google Scholar: [Author Only](#) [Title Only](#) [Author and Title](#)
- Gosa SC, Lupo Y, Moshelion M (2019)** Quantitative and comparative analysis of whole-plant performance for functional physiological traits phenotyping: New tools to support pre-breeding and plant stress physiology studies. *Plant Sci* 282: 49–59  
Google Scholar: [Author Only](#) [Title Only](#) [Author and Title](#)
- Grassi G, Magnani F (2005)** Stomatal, mesophyll conductance and biochemical limitations to photosynthesis as affected by drought and leaf ontogeny in ash and oak trees. *Plant, Cell Environ* 28: 834–849  
Google Scholar: [Author Only](#) [Title Only](#) [Author and Title](#)
- Haydon MJ, Mielczarek O, Robertson FC, Hubbard KE, Webb AAR (2013)** Photosynthetic entrainment of the *Arabidopsis thaliana* circadian clock. *Nature* 502: 689–692  
Google Scholar: [Author Only](#) [Title Only](#) [Author and Title](#)
- Hermida-Carrera C, Kapralov M V., Galmés J (2016)** Rubisco catalytic properties and temperature response in crops. *Plant Physiol* 171: 2549–2561  
Google Scholar: [Author Only](#) [Title Only](#) [Author and Title](#)
- Hetherington AM, Woodward FI (2003)** The role of stomata in sensing and driving environmental change. *Nature* 424: 901–908  
Google Scholar: [Author Only](#) [Title Only](#) [Author and Title](#)
- Janssens SB, Vandeloek F, De Langhe E, Verstraete B, Smets E, Vandenhouwe I, Swennen R (2016)** Evolutionary dynamics and biogeography of Musaceae reveal a correlation between the diversification of the banana family and the geological and climatic history of Southeast Asia. *New Phytol* 210: 1453–1465  
Google Scholar: [Author Only](#) [Title Only](#) [Author and Title](#)
- Jones H (1998)** Stomatal control of photosynthesis and transpiration. *J Exp Bot* 49: 387–398  
Google Scholar: [Author Only](#) [Title Only](#) [Author and Title](#)
- Jones HG (1985)** Partitioning stomatal and non-stomatal limitations to photosynthesis. *Plant, Cell Environ* 8: 95–104  
Google Scholar: [Author Only](#) [Title Only](#) [Author and Title](#)
- Kaiser E, Morales A, Harbinson J, Heuvelink E, Prinzenberg AE, Marcelis LFM (2016)** Metabolic and diffusional limitations of photosynthesis in fluctuating irradiance in *Arabidopsis thaliana*. *Sci Rep* 6: 1–13  
Google Scholar: [Author Only](#) [Title Only](#) [Author and Title](#)
- Kimura H, Hashimoto-Sugimoto M, Iba K, Terashima I, Yamori W (2020)** Improved stomatal opening enhances photosynthetic rate and biomass production in fluctuating light. *J Exp Bot* 71: 2339–2350  
Google Scholar: [Author Only](#) [Title Only](#) [Author and Title](#)
- Lawson T, Blatt MR (2014)** Stomatal size, speed, and responsiveness impact on photosynthesis and water use efficiency. *Plant Physiol* 164: 1556–1570  
Google Scholar: [Author Only](#) [Title Only](#) [Author and Title](#)
- Lawson T, Morison JIL (2004)** Stomatal function and physiology. *Evol. Plant Physiol. Elsevier*, pp 217–242  
Google Scholar: [Author Only](#) [Title Only](#) [Author and Title](#)
- Lobo F de A, de Barros MP, Dalmagro HJ, Dalmolin AC, Pereira WE, de Souza EC, Vourlitis GL, Rodríguez Ortiz CE (2013)** Fitting net photosynthetic light-response curves with Microsoft Excel - a critical look at the models. *Photosynthetica* 51: 445–456  
Google Scholar: [Author Only](#) [Title Only](#) [Author and Title](#)
- Matthews JSA, Viallet-Chabrand SRM, Lawson T (2017)** Diurnal variation in gas exchange: the balance between carbon fixation and water loss. *Plant Physiol* 174: 614–623  
Google Scholar: [Author Only](#) [Title Only](#) [Author and Title](#)
- McAusland L, Viallet-Chabrand S, Davey P, Baker NR, Brendel O, Lawson T (2016)** Effects of kinetics of light-induced stomatal responses on photosynthesis and water-use efficiency. *New Phytol* 211: 1209–1220  
Google Scholar: [Author Only](#) [Title Only](#) [Author and Title](#)
- Mencuccini M, Mambelli S, Comstock J (2000)** Stomatal responsiveness to leaf water status in common bean (*Phaseolus vulgaris* L.) is a function of time of day. *Plant Cell Environ* 23: 1109–1118  
Google Scholar: [Author Only](#) [Title Only](#) [Author and Title](#)
- Morales A, Kaiser E (2020)** Photosynthetic acclimation to fluctuating irradiance in plants. *Front Plant Sci* 11: 1–12  
Google Scholar: [Author Only](#) [Title Only](#) [Author and Title](#)
- Mott KA, Woodrow IE (2000)** Modelling the role of Rubisco activase in limiting non-steady-state photosynthesis. *J Exp Bot* 51: 399–406  
Google Scholar: [Author Only](#) [Title Only](#) [Author and Title](#)
- Outlaw WHJ (2003)** Integration of cellular and physiological functions of guard cells. *CRC Crit Rev Plant Sci* 22: 503–529  
Google Scholar: [Author Only](#) [Title Only](#) [Author and Title](#)
- Paine CET, Marthews TR, Vogt DR, Purves D, Rees M, Hector A, Turnbull LA (2012)** How to fit nonlinear plant growth models and

calculate growth rates: an update for ecologists. *Methods Ecol Evol* 3: 245–256

Google Scholar: [Author Only](#) [Title Only](#) [Author and Title](#)

Papanatsiou M, Petersen J, Henderson L, Wang Y, Christie JM, Blatt MR (2019) Optogenetic manipulation of stomatal kinetics improves carbon assimilation, water use, and growth. *Science* (80-) 363: 1456–1459

Google Scholar: [Author Only](#) [Title Only](#) [Author and Title](#)

Pearcy RW (1990) Sunflecks and photosynthesis in plant canopies. *Annu Rev Plant Physiol Plant Mol Biol* 41: 421–453

Google Scholar: [Author Only](#) [Title Only](#) [Author and Title](#)

Perrier X, De Langhe E, Donohue M, Lentfer C, Vrydaghs L, Bakry F, Carreel F, Hippolyte I, Horry J-P, Jenny C, et al (2011) Multidisciplinary perspectives on banana (*Musa* spp.) domestication. *PNAS* 108: 11311–11318

Google Scholar: [Author Only](#) [Title Only](#) [Author and Title](#)

Prioul JL, Chartier P (1977) Partitioning of transfer and carboxylation components of intracellular resistance to photosynthetic CO<sub>2</sub> fixation: A critical analysis of the methods used. *Ann Bot* 41: 789–800

Google Scholar: [Author Only](#) [Title Only](#) [Author and Title](#)

Qu M, Hamdani S, Li W, Wang S, Tang J, Chen Z, Song Q, Li M, Zhao H, Chang T, et al (2016) Rapid stomatal response to fluctuating light: an under-explored mechanism to improve drought tolerance in rice. *Funct Plant Biol* 43: 727

Google Scholar: [Author Only](#) [Title Only](#) [Author and Title](#)

**Raven JA (2014) Speedy small stomata? *J Exp Bot* 65: 1415–1424**

Resco de Dios V, Gessler A (2018) Circadian regulation of photosynthesis and transpiration from genes to ecosystems. *Environ Exp Bot* 152: 37–48

Google Scholar: [Author Only](#) [Title Only](#) [Author and Title](#)

Rudall PJ, Chen ED, Cullen E (2017) Evolution and development of monocot stomata. *Am J Bot* 104: 1122–1141

Google Scholar: [Author Only](#) [Title Only](#) [Author and Title](#)

Sakoda K, Yamori W, Shimada T, Sugano SS, Hara-Nishimura I, Tanaka Y (2020) Higher stomatal density improves photosynthetic induction and biomass production in *Arabidopsis* under fluctuating light. *Front Plant Sci*. doi: 10.3389/fpls.2020.589603

Google Scholar: [Author Only](#) [Title Only](#) [Author and Title](#)

Savitzky A, Golay MJE (1964) Smoothing and Differentiation of Data by Simplified Least Squares Procedures. *Anal Chem* 36: 1627–1639

Google Scholar: [Author Only](#) [Title Only](#) [Author and Title](#)

Slattery RA, Walker BJ, Weber APM, Ort DR (2018) The impacts of fluctuating light on crop performance. *Plant Physiol* 176: 990–1003

Google Scholar: [Author Only](#) [Title Only](#) [Author and Title](#)

Soleh MA, Tanaka Y, Kim SY, Huber SC, Sakoda K, Shiraiwa T (2017) Identification of large variation in the photosynthetic induction response among 37 soybean [*Glycine max* (L.) Merr.] genotypes that is not correlated with steady-state photosynthetic capacity. *Photosynth Res* 131: 305–315

Google Scholar: [Author Only](#) [Title Only](#) [Author and Title](#)

De Souza AP, Wang Y, Orr DJ, Carmo-Silva E, Long SP (2020) Photosynthesis across African cassava germplasm is limited by Rubisco and mesophyll conductance at steady state, but by stomatal conductance in fluctuating light. *New Phytol* 225: 2498–2512

Google Scholar: [Author Only](#) [Title Only](#) [Author and Title](#)

Taylor SH, Long SP (2017) Slow induction of photosynthesis on shade to sun transitions in wheat may cost at least 21% of productivity. *Philos Trans R Soc B Biol Sci*. doi: 10.1098/rstb.2016.0543

Google Scholar: [Author Only](#) [Title Only](#) [Author and Title](#)

Turner DW, Thomas DS (1998) Measurements of plant and soil water status and their association with leaf gas exchange in banana (*Musa* spp.): A laticiferous plant. *Sci Hortic (Amsterdam)* 77: 177–193

Google Scholar: [Author Only](#) [Title Only](#) [Author and Title](#)

Urban O, Šprtová M, Košvancová M, Tomášková I, Lichtenthaler HK, Marek M V. (2008) Comparison of photosynthetic induction and transient limitations during the induction phase in young and mature leaves from three poplar clones. *Tree Physiol* 28: 1189–1197

Google Scholar: [Author Only](#) [Title Only](#) [Author and Title](#)

Vialet-Chabrand S, Dreyer E, Brendel O (2013) Performance of a new dynamic model for predicting diurnal time courses of stomatal conductance at the leaf level. *Plant, Cell Environ* 36: 1529–1546

Google Scholar: [Author Only](#) [Title Only](#) [Author and Title](#)

Vialet-Chabrand SRM, Matthews JSA, McAusland L, Blatt MR, Griffiths H, Lawson T (2017) Temporal Dynamics of Stomatal Behavior: Modeling and Implications for Photosynthesis and Water Use. *Plant Physiol* 174: 603–613

Google Scholar: [Author Only](#) [Title Only](#) [Author and Title](#)

Vico G, Manzoni S, Palmroth S, Katul G (2011) Effects of stomatal delays on the economics of leaf gas exchange under intermittent light regimes. *New Phytol* 192: 640–652

Google Scholar: [Author Only](#) [Title Only](#) [Author and Title](#)



Wachendorf M, Küppers M (2017) The effect of initial stomatal opening on the dynamics of biochemical and overall photosynthetic induction. *Trees - Struct Funct* 31: 981–995

Google Scholar: [Author Only](#) [Title Only](#) [Author and Title](#)

Way DA, Pearcy RW (2012) Sunflecks in trees and forests: From photosynthetic physiology to global change biology. *Tree Physiol* 32: 1066–1081

Google Scholar: [Author Only](#) [Title Only](#) [Author and Title](#)

van Wesemael J, Kissel E, Eyland D, Lawson T, Swennen R, Carpentier S (2019) Using growth and transpiration phenotyping under controlled conditions to select water efficient banana genotypes. *Front Plant Sci* 10: 1–14

Google Scholar: [Author Only](#) [Title Only](#) [Author and Title](#)

Weyers JDB, Johansen LG (1985) Accurate estimation of stomatal aperture from silicone rubber impressions. *New Phytol* 101: 109–115

Google Scholar: [Author Only](#) [Title Only](#) [Author and Title](#)

Wilson KB, Baldocchi DD, Hanson PJ (2000) Quantifying stomatal and non-stomatal limitations to carbon assimilation resulting from leaf aging and drought in mature deciduous tree species. *Tree Physiol* 20: 787–797

Google Scholar: [Author Only](#) [Title Only](#) [Author and Title](#)

Yamori W, Kusumi K, Iba K, Terashima I (2020) Increased stomatal conductance induces rapid changes to photosynthetic rate in response to naturally fluctuating light conditions in rice. *Plant Cell Environ* 43: 1230–1240

Google Scholar: [Author Only](#) [Title Only](#) [Author and Title](#)